Journal of Applied Meteorology and Climatology

Evaluation of Modeled Lake Breezes Using an Enhanced Observational Network in Southern Ontario: Case Studies

--Manuscript Draft--

Manuscript Number:	JAMC-D-17-0231
Full Title:	Evaluation of Modeled Lake Breezes Using an Enhanced Observational Network in Southern Ontario: Case Studies
Article Type:	Article
Order of Authors:	Armin Dehghan
	Zen Mariani
	Sylvie Leroyer
	Paul Joe
	David Sills
	Stephane Belair
Manuscript Classifications:	3.328: Sea breezes; 5.116: Remote sensing; 5.140: Surface observations; 8.116: Model evaluation/performance
Abstract:	Canadian Global Environmental Multiscale (GEM) numerical model output was compared to the meteorological data from an enhanced observational network in order to investigate the model's ability to predict Lake Ontario lake breezes and their characteristics for two cases in the Greater Toronto Area (GTA) - one under opposing wind and another under non-opposing wind. The enhanced observational network of surface meteorological stations, a C-band radar and two Doppler wind lidars were deployed among other sensors during 2015 Pan/Parapan Games in Toronto. The GEM model was run for three nested domains with grid spacings of 2.5, 1 and 0.25 km. Comparisons between the model predictions and ground-based observations showed that the model successfully predicted lake breezes for the two events. The results indicated that using GEM 1 and 0.25 km increased the forecast accuracy of the lake-breeze location, updraft intensity and depth. The accuracy of the modeled lake breeze timing was approximately ±90 minutes. The model under-predicted the surface cooling caused by the lake breeze. The GEM 0.25 km model significantly improved the temperature forecast accuracy during the lake-breeze circulations, reducing the bias up to 72%, but it mainly under-predicted the moisture and over-predicted the surface wind speed. Root Mean Square Errors of wind direction forecasts were generally high due to large biases and high variability of errors.

Evaluation of Modeled Lake Breezes Using an Enhanced Observational Network in Southern Ontario: Case Studies

Armin Dehghan[1], Zen Mariani[1], Sylvie Leroyer[2], Paul Joe[1], David Sills[1] and Stéphane Bélair[2]

[1]Observation-Based Research Section, Environment and Climate Change Canada, Toronto, Canada
[2]Environmental Numerical Prediction Research, Environment and Climate Change Canada, Dorval, Canada

Abstract:

Canadian Global Environmental Multiscale (GEM) numerical model output was compared to the meteorological data from an enhanced observational network in order to investigate the model's ability to predict Lake Ontario lake breezes and their characteristics for two cases in the Greater Toronto Area (GTA) – one under opposing wind and another under non-opposing wind. The enhanced observational network of surface meteorological stations, a C-band radar and two Doppler wind lidars were deployed among other sensors during 2015 Pan/Parapan Games in Toronto. The GEM model was run for three nested domains with grid spacings of 2.5, 1 and 0.25 km. Comparisons between the model predictions and ground-based observations showed that the model successfully predicted lake breezes for the two events. The results indicated that using GEM 1 and 0.25 km increased the forecast accuracy of the lake-breeze location, updraft intensity and depth. The accuracy of the modeled lake breeze timing was approximately ±90 minutes. The model under-predicted the surface cooling caused by the lake breeze. The GEM 0.25 km model significantly improved the temperature forecast accuracy during the lake-breeze circulations, reducing the bias up to 72%, but it mainly under-predicted the moisture and over-predicted the surface wind speed. Root Mean Square Errors of wind direction forecasts were generally high due to large biases and high variability of errors.

Corresponding Author: Armin Dehghan, armin.dehghan@canada.ca

1. Introduction

The 2015 Pan American and Parapan American Games from July 10 to August 15 provided Environment and Climate Change Canada (ECCC) with a unique opportunity to undertake an extensive observation campaign in the Greater Toronto Area (GTA) including a mesoscale network specifically designed to detect and track lake breezes (Joe et al. 2017). Additionally, two Doppler lidars (hereafter referred to as lidars) provided real-time observations of winds. The Canadian Global Environmental Multiscale (GEM) numerical model was run at the horizontal grid spacings of 2.5, 1 and 0.25 km to study its ability to predict lake breezes.

Lake breezes develop due to the temperature contrast between the lake water and land surface (Atkinson 1981; Pielke 1984). The thermal contrast produces a pressure difference between the lake and land that forces cooler air inland off the lake. Fig. 2 of Sills et al. (2011) shows an idealized lake breeze circulation. The lake-breeze front develops at the leading edge of the inflow layer. The surface convergence and updraft at the lake-breeze front can generate a narrow band of convective clouds (Hasti et al. 1999). The altitude of the return flow above the inflow layer indicates the depth of the lake-breeze circulation, typically from 100 m to 1000 m (Lyons 1972; Keen and Lyons 1978; Curry et al. 2016; Mariani et al. 2017).

The GTA is often affected by lake breezes due to vicinity to Lake Ontario. Estoque et al. (1976) investigated the structure and diurnal variations of lake breezes over the southern part of the Lake Ontario using both observational and numerical simulations. The passage of the lake-breeze front was marked by a sharp shift in wind direction, decrease in temperature, and increase in relative humidity. Estoque et al. (1976) also showed that the lake-breeze front depth can reach 250 m, and they can penetrate as far as 30 km inland. Comer and McKendry (1993) extended the work of Estoque et al. (1976) by investigating a wider range of data. They used the lake-breeze index developed by Biggs and Graves (1962) to identify lake breezes. It was found that lake breezes develop over 30% of the days during summer over Lake Ontario and can penetrate as far as 45 km inland. They also suggested that the wind field over Lake Ontario can be influenced significantly by nearby lakes. In the more recent studies of lake breezes in the GTA, it was found that GTA lake breezes occurred on more than 70% of warm season days (Wentworth et al. 2015; Mariani et al. 2017).

The lake-breeze studies in southern Ontario have shown that the lake-breeze fronts can penetrate far inland to distances up to 215 km (Sills et al. 2011), initiate thunderstorms (Sills et al. 2002; King et al. 2003) and affect air quality (Hastie et al. 1999; Hayden et al. 2011; Wentworth et al. 2015). Lake breezes have large effects on the coastal cities particularly in spring and summer, and it is therefore important to forecast lake-breeze fronts accurately.

Previous modeling studies of Lake Ontario lake breezes are limited to numerical models with grid spacings of 20 and 10 km (Estoque and Gross 1981; Comer and McKendry 1993). Estoques and Gross (1981) used a primitive equation model (e.g., momentum, thermodynamic continuity equations) with variable grid spacings of 20 km (along x axis of domain) and 10 km (along y axis of domain) and five vertical levels. They compared the simulated lake breeze with observations for one day. Their results showed that the effect of prevailing flows and orography were important in simulating the characteristics of the lake breeze. The comparison of the simulated and observed lake-breeze front showed a general agreement. It was suggested that the detailed differences (e.g., lake breeze location and convergence zone) were due to deficiencies of the model equations, unrealistic initial conditions and a flat terrain. Comer and McKendry (1993) simulated the Lake Ontario breezes using the Colorado State University (CSU) mesoscale model with grid spacings of 40 km for the main domain and 10 km for the nested domain. Simulations with four different gradient wind directions showed generally good agreement with observations. However, the model underestimated the inland penetration of lake breezes. They also showed that the Lake Ontario lake breeze was strongly influenced by the size and shape of the Lake as well as the large-scale wind direction.

Sills et al. (2011) identified the lake-breeze fronts using GEM 2.5 km simulations over the Great Lakes. The model showed some ability to predict lake breezes successfully. However, the timing and locations of the lake-breeze fronts did not match the observations in detailed case studies over the Lake Erie, Lake St. Clair and Lake Huron. The Lake Ontario and Toronto region were not included in their study. Leroyer et al. (2014) studied the sea-breeze events around the urban coastal area of Vancouver using GEM with grid spacings of 2.5, 1 and 0.25 km. Results showed that although GEM 2.5 and 1 km provided accurate near-surface meteorological variables (e.g., temperature, wind speed and wind direction), the physical processes involved with sea-breeze fronts (e.g., sea-breeze inland penetration, interaction with large-scale flow) were handled better with GEM 0.25 km. Kehler et al. (2016) examined 56 cases of lake breezes over Lake Winnipeg and Lake Manitoba. They showed that GEM 2.5 km correctly simulated 78% and 68% of the Lake Winnipeg and Lake Manitoba lake breeze occurrences, respectively.

During the Pan/Parapan American games, in addition to observations, the experimental high-resolution GEM 1 and 0.25 km were run semi-operationally for the first time for the GTA and Lake Ontario to support the weather forecast program and to evaluate the high-resolution GEM forecasts. Mariani et al. (2017) demonstrated that synoptic winds had an important impact on the characteristics of the lake-breeze fronts in the GTA during the games. Thus, the main objective of this paper is to test the ability of the GEM model to predict Lake Ontario lake breezes under different synoptic winds in two cases, and to determine if increasing the model spatial resolution improves the forecast of lake-breeze characteristics. The ground-based observational network is used to verify the accuracy of predicted temperature, dew point temperature, wind speed and wind direction. The data, model design and lake-breeze identification methods are presented in Section 2. The model simulations of lake breezes and characteristics of lake-breeze fronts, including comparison to ground-based observations, and discussions are provided in Section 3. The conclusions are given in Section 4.

2. Data and methodology

a. Doppler lidar data

Doppler lidars provide high-resolution (3 m) radial velocity measurements of wind by measuring the Doppler shift of the backscattered laser from aerosols. This allows remote observation of the horizontal and vertical structure of lake-breeze circulations at high resolution. (Darby et al. 2002; Tsunematsu et al. 2009; Mariani et al. 2017). During the 2015 Pan/Parapan American Games, two scanning lidars operated in constant elevation (Plan Position Indicator; PPI), constant Azimuth (Range Height Indicator; RHI) and vertically staring modes. One of the lidars was deployed at Hanlan’s Point (43° 36' 44" N, 79° 23' 19" W) on Toronto Island and operated continuously. The second lidar was mounted on the back of a pick-up truck and driven to different locations within the GTA, and tracked the lake-breeze front as it transited northward. The maximum range of the lidars measurements was variable depending on weather conditions typically changing from 2 to 5 km. The lidar measurements conducted at Hanlan’s Point and Highway 400 ONroute (43° 53' 38" N, 79° 33' 26" W) will be used in this study.

b. Mesonet data

During the 2015 Pan/Parapan American Games, 53 automated surface weather stations were added to the existing network. This mesoscale network, or “mesonet”, provided weather information including temperature, dew point, relative humidity, air pressure, wind speed and direction, precipitation, and air quality data at different locations across the GTA. The weather stations were set up on or near transects perpendicular to the lakeshore in order to track the inland penetration of the lake-breeze fronts (Joe et al. 2017). The tower stations measured wind at 10 m and temperature and dew point at 1.5 m (Above Ground Level; AGL) except at the North York location where the tower was installed at top of a low-rise building. The compact stations were deployed to increase the network spatial density. Half of the compact stations (20 stations) were installed on top of low-rise buildings. The compact stations used all-in-one sensors while the towers used research-grade sensors. Table 1 shows the heights and types of the observational stations of this study. Note that the compact stations were installed at different sides of the rooftops. This could affect the measurements depending on the wind direction and the location of sensors on the rooftops. The compact stations data were lightly quality controlled to remove the out of bound values. The tower data were quality controlled thoroughly. The compact and tower stations provided data as 1-min averages.

c. Doppler radar data

The operational C-band Doppler radar in this study was located north of Toronto in King City (43° 57' 50'' N, 79° 34' 26'' W). The radar operated at 5625 MHz frequency with a beamwidth of 0.62°. The temporal and spatial resolution of the radar is 10 min and 125 m, respectively. The radar is capable of making measurements at a distance as far as 250 km (Hudak et al. 2006;

Boodoo et al. 2010). These measurements cover the GTA and Lake Ontario. Radar “fine lines” are often observed and are due to the presence of insects along the updrafts of lake-breeze fronts and other mesoscale boundaries. The radar fine lines can be used along with other observations to track lake-breeze fronts (Sills et al. 2011).

d. GEM model data

The GEM atmospheric model was originally developed in the 1990s at ECCC (GEM; Côté et al. 1998; Zadra et al. 2008). It is based on a fully implicit temporal solution on staggered vertical and horizontal grids (Girard et al. 2014). A full suite of physical processes is represented in the GEM model (Bélair et al., 2003a, b). The configuration of the model included three nested domains with grid spacings of 2.5, 1 and 0.25 km (see Fig. 1) and 57 vertical levels. The output of the Regional Deterministic Prediction System (RDPS; Fillion et al. 2010) with a grid spacing of 10 km provided initial and hourly boundary-layer conditions to the 2.5 km domain. A summary of physics schemes, time steps, horizontal grid spacing and vertical levels is provided in Table 2. In order to simulate the lake-breeze flows, accurate differential heating between the lake and the land is required. Therefore, surface temperatures for the Great Lakes were prescribed using 2 km hourly output from a coupled ocean-atmosphere forecasting system (Dupont et al. 2012) for this study. For the remaining water bodies over the model domains, direct output from the 10 km RDPS and analyses based on buoys and satellite data (Brasnett 2008) were used. Turbulent fluxes over the water were estimated using the aerodynamic roughness length of Charnock (1955). Furthermore, the thermal and humidity roughness length of Deacu et al. (2010) was used since it improved the simulation of fluxes over the Lake Ontario. The model also used the advanced double-moment microphysics scheme of Milbrandt and Yau (2005). The land surface model of the interaction between surface, Biosphere and Atmosphere

(ISBA, Noilhan and Planton 1989; Bélair et al. 2003a, b) and Town Energy Balance (TEB; Masson 2000) represented land surface physical processes over natural and urban land surfaces, respectively. The details of the model configuration and parameterization schemes are described by Leroyer et al. (2014).

e. Lake-breeze identification methods

Mesoscale analysis described in Sills et al. (2011), used mesonet data including temperature, dew point, wind speed and wind direction measurements, satellite images from GOES13, and the C-band radar reflectivity to identify the lake-breeze front. The criteria for a lake breeze observation are identified in Table 1 in Sills et al. (2011). These include the observation of a sharp change in wind speed, onshore winds, a sharp decrease in temperature, an increase in dew point, a line of cumulus clouds from satellite images, and a radar fine line. When all data were available, the mesoscale analysis error associated with the lake-breeze front position was ± 1km.

The GEM forecasts of a wind direction shift (~10 m AGL), decrease in temperature (~5 m AGL) and increase in dew point (~5 m AGL) were used to identify lake breezes at 15 minute intervals. Additionally, the predicted vertical velocities were analyzed since when enhanced they could be an indicator of a lake-breeze front (Harris and Kotamarthi 2005; Sills et al. 2011). The vertical velocities at ~120 m (AGL) were used in order to minimize near-surface effects.

3. Results and discussions

The mesoscale analyses over the GTA indicated that the lake-breeze front on July 15, 2015 was slow-moving with limited maximum inland penetration of 6 km under a north-easterly synoptic wind (opposing flow). The front remained inland from the shore for ~10 hours before it decayed. In contrast, the lake-breeze front on August 9, 2015 was fast-moving, traveling more than 60 km inland within ~5 hours under easterly/north-easterly synoptic winds (non-opposing flow). The primary purpose of this section is to determine whether the high-resolution GEM model predicted the characteristics and impact of the lake-breezes under the two different synoptic flows.

a. Lake-breeze events

Surface high pressure dominated the GTA with north-easterly synoptic flow (offshore) on July 15, 2015. The maximum temperature reached 21.9°C at Toronto international airport. The mesoscale analysis showed that the surface wind shifted to south/south-westerly as the lake-breeze front passed the lakeshore at 15:08 UTC. The lake-breeze front traveled 6 km inland before it began to retreat lakeward at 20:00 UTC. On August 9, the easterly/ north-easterly synoptic flow was dominant throughout the day. The Toronto international airport recorded the maximum temperature of 24.2°C. Mesoscale analyses showed that the lake-breeze front developed at the eastern part of the lakeshore at 14:00 UTC and extended to the western part of the GTA by 15:00 UTC. The lake-breeze front reached its maximum distance in the GTA at 23:00 UTC.

Figs. 2-4 show examples of mesoscale and GEM model output analyses used for identification of lake-breeze fronts on July 15 and August 9. Fig. 2a illustrates that the observed wind was north-easterly ahead of the lake-breeze front at 21:00 UTC on July 15 UTC in the GTA. This was captured by GEM 0.25 km, which predicted north-easterly/north-westerly winds in Fig. 3b. The predicted vertical velocity plot for July 15 (Fig. 3a) shows that the model generated a narrow updraft zone parallel to the lakeshore coinciding with wind shifts to onshore, decrease in wind speed (Fig. 3b), decrease in temperature (Fig. 3c) and increase in dew point (Fig. 3d). The position of the updraft zone was similar to the position of observed lake-breeze front (magenta line in Fig. 3).

The mesoscale analyses identified the lake-breeze front on August 9 at 15:00 UTC in the GTA (Fig. 2b). However, due to the onshore synoptic-scale flow, gradients along the front were markedly weaker and the front was less well-defined in satellite and radar imagery than was the case for July 15. The leading edge of the lake breeze in the GEM 0.25 km model output was even less defined, with no discernable updraft zone in the analysis of vertical velocity (Fig. 4). Instead, the model predicted a series of convective rolls in the GTA. The model also produced more turbulent boundary-layer flow deeper inland (depicted in the upper portion of the Figs 4a-b) and more uniform boundary-layer flow close to the Lake Ontario. This suggests that the model likely predicted the suppressing effect of the relatively cool marine air on thermal developments. The model also predicted a decrease in temperature and an increase in dew point only in areas close to the lakeshore, not along the leading edge of the lake breeze.

b. Lake-breeze front characteristics

1) Inland penetration

The inland penetration distance of the Lake-breeze front was examined using the interpolation of vertical velocity along the shore-A2T cross-section (red line in Figs. 3a-4a). Figs 5-6 show the cross-section of vertical velocities for July 15 and August 9, respectively. The intersections of the observed lake-breeze fronts (mesoscale analyses) with the cross-section were also determined and marked in Figs. 5-6.

The predicted vertical velocity maxima in Fig. 5 clearly illustrated that the updraft zone moved inland slowly on July 15 and returned to the lakeshore in agreement with mesoscale analyses.

However, the predicted updraft zone of maximum vertical velocity with GEM 0.25 km was not continuous since the model tended to resolve smaller structures of updrafts and downdrafts. This was more evident in the August 9 case since the high-resolution model produced more thermals.

On August 9, GEM 0.25 km produced two different regimes of vertical motions in Fig. 6c; one with smaller updraft structures ahead of the observed lake-breeze front and another with elongated structures behind the observed lake-breeze front. Even though the Fig.7 illustrated the wind shift of north-easterly flow to south-easterly, the updraft zone of lake-breeze front was not clear (Fig. 6c). It appears that the GEM 0.25 km model predicted the lake-breeze circulation at the lakeshore (Fig. 4) but it failed to generate enough convergence along the leading edge of the lake breeze. Nevertheless, the GEM 0.25 km model failed to generate a clear lake-breeze frontal zone possibly due to misrepresentation of convection at thermals and the frontal zone.

The results also showed that the magnitude of vertical velocity increased for GEM 1 and 0.25 km (Leroyer et al. 2014) in both cases, while the width of the updraft zone decreased. The width of the updraft zone was defined as the width of the enhanced vertical velocity zone. As a result, GEM 0.25 km produced an updraft zone with a width of less than 2 km on July 15. Lake-breeze fronts are generally less than 2 km in width (Lyons 1972; Curry et al. 2016). Hence, GEM 0.25 km represented the lake-breeze width better in this case.

The distance traveled by the predicted lake breeze was determined by locating the maximum vertical velocity in the updraft zone (Fig. 8). The GEM 0.25 km model failed to generate the updraft zone of lake-breeze front on August 9, but it appears that the model predicted the changes in temperature, dew point and wind due to advected marine air by the onshore synoptic flow. Hence, the maximum vertical velocity in thermals at the boundary between two turbulent flows was used to study the impact of the GEM 0.25 km prediction of lake breeze on August 9. The results were compared to the inland penetration of the lake-breeze fronts identified by mesoscale analysis. While the observed lake-breeze front reached its maximum distance from the lakeshore (~6 km) at 20:00 UTC on July 15, the predicted lake-breeze fronts with GEM 2.5 and 1 km reached the maximum distance of 2.2 and 2.8 km at 17:00 UTC and 19:00 UTC, respectively. The predicted lake-breeze front with GEM 0.25 km penetrated to maximum 5.6 km at 22:00 UTC before it returned to lakeshore. The model generally underestimated the inland penetration in this case. The average differences between the predicted and observed inland penetrations from 17:00 to 23:00 UTC, were 2.3, 2.4 and 0.9 km for GEM 2.5, 1 and 0.25 km, respectively. On August 9, the model initially underestimated the inland penetrations but the predicted lake-breeze front traveled deeper inland than observed after one hour (Fig. 8b). The averaged differences between the predicted and observed lake-breeze front penetrations from 15:00 to 17:30 UTC were 2.4 and 1.6 km with GEM 2.5 and 1 km, respectively. The averaged difference between the predicted lake breeze advection with GEM 0.25 km and observed lake-breeze front penetration was 4 km for the August 9 case. Overall, the location of the lake-breeze front was predicted more accurately with GEM 0.25 km on July 15 and with GEM 1 km on August 9.

2) Updraft intensity

The intensity of the lake-breeze updraft was determined by measuring the maximum vertical velocity. The lidar analyses showed that the lake breeze impacted Hanlan's Point from 14:00 UTC on July 15 until 00:00 UTC on July 16 (Mariani et al. 2017). Fig. 9 shows the vertical profiles of vertical velocities at the Hanlan's Point site for this period of time. The positive (updraft) and negative (downdraft) vertical velocities measured by lidar (Fig. 9a), were associated with convective mixing in the atmospheric boundary layer. Lidar measurements exhibited an increase of updraft intensity at 14:23-14:31 UTC extending from surface to about 600 m above surface. The maximum vertical velocity of 2.3 ms^{-1} was measured at 14:27 UTC at the altitude of 310 m. Furthermore, the lidar PPI scan of Lake Ontario (Fig. 10a) at 14:24 UTC showed that the air flow direction changed from offshore to onshore, indicating the passage of lake-breeze front. The predicted vertical velocities are presented in Figs. 9(b)-(c) for the same period of time. The GEM 2.5, 1 and 0.25 km predicted that the maximum vertical velocity occurred later at 16:45, 16:00 and 16:00 UTC, respectively. Similar to Fig. 5, by increasing the model resolution, the updraft zone narrowed and the vertical velocities increased. The maximum vertical velocities of 0.2 and 0.5 ms^{-1} were predicted with GEM 2.5 and 1 km, respectively. These values are significantly smaller than the lidar observation of the lake-breeze updraft. The GEM 0.25 km predicted higher vertical velocity of 1.9 ms^{-1} at 365 m. This suggests that the increase of model resolution (grid spacings of 0.25 km) increased the accuracy of the updraft intensity prediction, though it did not improve the accuracy of the updraft timing in this case.

The profiles of vertical velocity for the August 9 case at the Highway 400 ONroute site are presented in Figs. 11-12. The mobile lidar operated from 18:00 to 21:00 UTC at this location with a limited range of measurements. The maximum vertical velocity of 3.3 ms^{-1} was measured at 18:19 UTC at an altitude of 230 m (Fig. 11a and 12). Additionally, the PPI scan in Fig. 10b illustrated that the wind shifted to onshore flow at 18:14 UTC, indicating the passage of lake-breeze front. The predicted vertical velocities in Figs. 11b-c for the period of 18:00 to 21:00 UTC showed that maximum vertical velocities of 0.16, 0.75 and 2.1 ms^{-1} were predicted at 760, 760 and 680 m with GEM 2.5, 1 and 0.25 km, respectively. The maximum vertical velocity with GEM 0.25 km was likely associated with thermals updraft since no lake-breeze front was predicted in this case. However, the order of magnitude of lidar maximum vertical velocity for the available measurements (Fig. 12) was more comparable to the GEM 0.25 km prediction of vertical velocity for this case. The timing of the maximum vertical velocity did not change significantly for different resolution of the model.

3) Depth

The RHI scans taken at Hanlan's Point and Highway 400 ONroute (Fig. 13) were used to find lake-breeze depths by locating the altitude where the direction of radial velocity changed from onshore to offshore. Similarly the modeled lake-breeze depth was estimated by locating the altitude at which the horizontal velocity shifted to offshore wind. Fig. 14 shows the observed and predicted lake-breeze depths for July 15 and August 9. The results in Fig. 14a indicated that the depth increased after the lake-breeze front passage at 14:24 UTC on July 15, and decreased after the lake breeze dissipated at Hanlan's Point. The comparisons between GEM output and lidar-measured depth showed that the model did not generate any lake-breeze depth until 16:15 UTC due to the late lake-breeze front model timing. The model underestimated the lake-breeze depth on average by 83, 37 m with GEM 2.5 and 1 km, respectively, and overestimated by 27 m with GEM 0.25 km from 16:30 to 23:15 UTC.

On August 9, GEM 2.5, 1 and 0.25 km overestimated the depth by 255, 133 and 143 m, respectively from 18:15 to 20:45 UTC. While the GEM predictions of the lake-breeze depth were generally larger than observations (Fig. 14b), GEM 0.25 km predicted closer values to the observations within 45 minutes from the time the observed lake-breeze front passed over the lidar site at ~18:15 UTC. The GEM 0.25 km initially underestimated the depth by 28 m from 18:30 to 19:00 UTC, but the error increased after 19:00 UTC. One should note that both measured and predicted lake-breeze depths on this day were larger than depths on July 15 likely due to greater low-level instability in the atmosphere which could encourage an extension of the lake breeze vertical structure (Atkinson 1981).

Overall, GEM 1 and GEM 0.25 km performed better in predicting the lake-breeze depth for the two events. Both the measured and predicted lake-breeze depths were within the ranges (100-1000) of previous studies of lake-breeze depth (Lyons 1972; Curry et al. 2016).

c. Lake-breeze front impact

Time series of 1-minute observations at selected surface stations (Table 2) are used to examine the accuracy of the predicted temperature drop, dew point rise, horizontal wind speed decrease and timing of wind shift to onshore upon arrival of the lake-breeze front. The wind shift timing of 1-minute data was selected to match the timing on the mesoscale analyses. The decrease in temperature and increase in dew point were estimated from 15 minutes before the wind shift until 45 minutes after, since the change in temperature and dew point can begin earlier than wind shift. Similar method was used to analyze the model output. Note that the lake-breeze front was not clearly predicted with the GEM 0.25 km model in August 9, therefore the impact due to the propagation of marine air inland was considered in this particular case. The results are presented in Table 3. The decrease in wind speed due to lake-breeze front is not included in the table since it was only observed on July 15 at Z2D and L1B. Figs. 15-16 show the time series of temperature, dew point, wind direction and wind speed at Z2D station for July 15 and August 9, respectively.

On July 15, the temperature dropped 1.3°C and the dew point rose 1.6°C at 15:08 UTC at Z2D. The offshore wind (1°-90° and 270°-360°) also shifted to onshore wind (90°-270°) and wind speed decreased by ~2 ms^{-1} indicating that lake-breeze arrived at the station. Comparisons of the GEM outputs with observations showed that the model failed to capture the sharpness of wind direction changes possibly due to diffusive processes in the model. The model also predicted a smaller drop in temperature at 16:15-16:30 UTC. A maximum temperature decrease of 0.9°C and maximum dew point increase of 0.7°C were predicted by the model. The ground-based observations also showed that the lake-breeze front reached the L1B site at 18:45 UTC and remained quasi-stationary until 20:30 UTC causing a temperature drop of 2.3°C, dew point rise of 3°C and wind speed decrease of 0.9 ms^{-1}. The lake-breeze front returned slowly arriving at the lakeshore at 00:00 UTC on July 16. The model predicted a similar pattern though it could not propagate the front to the L1B station (see Fig. 5). As a result, the model did not predict any wind shift or temperature decrease (except with GEM 0.25 km), but predicted the increase in dew point.

The temperature and dew point values were higher at Z2D on August 9 compared to July 15 for the period of 12:00 UTC to 00:00 UTC. Observations also showed a decrease of 1.4°C in temperature, an increase of 1.1°C in dew point and a change of wind direction from offshore to onshore at ~14:42 UTC; no sharp changes in wind speed was observed at Z2D possibly due to rapid propagation of the lake-breeze front. The model predicted the maximum temperature drop and dew point increase of 0.2°C and 0.3°C, respectively for this station.

The model consistently underestimated the temperature drop associated with the lake-breeze front at all the examined cases in this study. The errors of the predicted temperature drops ranged 0.4-2.5°C and reduced up to 30% by increasing the model resolution except at Z2D. The model also underestimated the increase in dew point up to 2.1°C. The predicted lake-breeze front (wind shift) timing was late by maximum 82 minutes for stations close to lakeshore and early by maximum 98 minutes for stations located deep inland. The increase of model resolution improved the prediction accuracy of timing only at some stations.

d. Near-surface meteorological variables

The predicted temperature, dew point, wind direction and horizontal wind speed were compared to ground-based observations to evaluate the performance of the model from the time the lake-breeze fronts arrived at the surface station until the time the lake-breeze circulations ended. Following the approach in Sills et al. (2011), the end time was defined as the last hour that the lake breeze could be seen on the lakeshore. Therefore, the time at which the wind shifted to offshore was considered as the end time of the lake-breeze circulation. For example, on July 15, the model was evaluated at Z2D from the arrival time of lake-breeze front at 15:08 UTC until the end of the circulation at 01:00 UTC on July 16.

Figs. 17-18 show the Mean Bias Error (MBE) and Standard Deviation of Error (STDE) estimated at 15 minutes intervals on July 15 and August 9. The model data at the first prognostic level (~10 m for wind and ~5 m for temperature and dew point) was used for calculating the metrics since this was the nearest level to the altitudes of observations (2.5-10.3 m AGL). In addition, the lake-breeze circulation timing during which the metrics were calculated varied depending on the lake-breeze front arrival time. Therefore, the errors at surface stations can-not be compared directly. Nevertheless, the focus of this section is to obtain a range of errors during the lake-breeze events rather than comparing the results of different surface stations.

The results indicated that the GEM 2.5 km model underestimated temperature by 1.4-3.6°C in both case studies at all the selected stations. It also overestimated the dew point by 0.6-3°C except at Z2D and A2T stations. The wind direction MBEs were high ranging from 9° to 93°. The wind direction errors were particularly large at L1B on July 15 since no lake-breeze front was predicted for the L1B station. The predicted wind direction remained offshore during most of the day at this location leading to large errors during the lake-breeze circulation. The wind speed was overestimated on July 15 and underestimated on August 9 with GEM 2.5 km. The wind speed MBE ranged from 0.1 to 2.2 ms^{-1} with GEM 2.5 km. The increase of model resolution (grid spacings of 1 and 0.25 km) improved the accuracy of temperature prediction, reducing the MBE up to 72%. GEM 1 and 0.25 km mostly underestimated the dew point and overestimated the wind speed. The MBEs of dew point and wind speed were reduced at some stations up to 86% with GEM 1 and 0.25 km. The increase of model resolution did not reduce the wind direction MBE significantly, except at L1B on July 15. The results also showed that the wind direction errors had the highest variability (STDE) compared to temperature, dew point and wind speed. This was expected due to natural variability of wind direction and inability of numerical models to accurately capture these variabilities and the timing of wind shifts (Hanna 1994; Harris and Kotamarthi 2005).

The forecast accuracy was determined by estimating Root Mean Square Errors (RMSE). The RMSE values of temperature, dew point, wind direction and wind speed ranged over 0.6-3.6°C, 0.7-3.1°C, 21°-195° and 0.6-2.4 ms^{-1}, respectively. In order to find the confidence interval of RMSE values, the bootstrap method (DiCiccio and Efron 1996) was used. The method is based on resampling with replacement from the given sample. For this work, the errors (forecast-observation) were resampled 10000 times. The RMSE of resampled errors was calculated, and the 10% and 90% percentile of the RMSEs distribution were estimated for the confidence intervals. The results are presented in Figs. 19-20. The forecast accuracy of temperature improved significantly at all the selected stations when the model resolution increased (grid spacings of 1 and0.25 km) leading to decrease of RMSE by maximum 66%. The forecast accuracy of dew point, wind direction and speed improved at some stations.

4. Conclusions

This study explores the ability of the GEM model to forecast the lake breezes under opposing and non-opposing synoptic flows during the 2015 Pan/Parapan American games in Toronto. The case studies included the July 15 event where a slow-moving lake-breeze front impacted the GTA lakeshore regions for ~10 hours and the August 9 event where a fast-moving lake-breeze front penetrated more than 60 km inland through the GTA in ~6 hours. The modeled lake breezes were compared with mesoscale analyses, lidar observations of radial winds, and surface stations observations. The followings were found:

(i) The GEM model successfully predicted the lake-breeze fronts for the two lake-breeze events, except when using 0.25 km horizontal grid spacing for the August 9th onshore synoptic-scale flow case. The wind direction shifts to onshore were captured by the model as were the decrease and increase in simulated temperature and dew point, respectively.

(ii) The predicted vertical velocity with GEM 2.5 and 1 km clearly showed the lake-breeze frontal zone for the two events, however, the frontal zone predicted with GEM 0.25 km did not have associated enhanced updrafts on August 9. It seems that the model failed to adequately represent the updrafts at both thermals and the frontal zone, and instead produced several convective rolls. We speculate that the representation of turbulence in the model contributed to this issue.

(iii) GEM 0.25 km generated elongated, weak updraft structures in the lake breeze inflow region that were approximately aligned with the onshore surface wind for both July 15 and August 9.

This suggests that the high-resolution model likely captured the suppressing effect of the cooler lake air on the generation of thermals.

(iv) Comparisons of the predicted characteristics of lake-breeze fronts including inland penetration, updraft intensity, depth and timing with observations showed that GEM 2.5 km predicted the lake-breeze front characteristics with some degree of accuracy during the two events. However, the accuracy improved significantly when the model ran with the grid point spacings of 0.25 km for the July 15 case and with a grid point spacing of 1 km for the August 9 case.

(v) The model underestimated the cooling behind the lake-breeze front by up to 2.5°C in this study. It also underestimated the rise in dew point by up to 2.1°C. While the increase of model resolution improved the prediction of the temperature drops at all the selected locations, it improved the dew point increases prediction at some locations. In addition, the model sometimes failed to capture the sharpness of changes in the wind direction during the passage of lake-breeze front, possibly due to diffusion processes in the model.

(vi) During the lake-breeze circulation defined as the time the lake-breeze front arrived at surface stations until it decayed, the model underestimated the temperature up to 3.6°C. While GEM 2.5 km overestimated the dew point by maximum 3°C, GEM 1 and 0.25 km underestimated the dew point up to 1.3°C. The GEM 2.5 km model also underestimated the wind speed while the higher-resolution model overestimated up to 2 ms^{-1}. The biases and variability of errors for wind direction predictions were generally very high.

(vii) During the lake-breeze circulation, the increase of model resolution increased the accuracy of temperature predictions significantly within 90% percentile at all the selected stations.

However, it improved the accuracy of dew point, wind speed and direction predictions at some of the selected stations.

There are several aspects of the atmospheric model that need to be examined in order to improve the representation of lake-breeze circulations over the GTA. For instance, how much would better modeling of lake surface temperatures improve the GEM's performance? Is the turbulent exchange between the Lake Ontario and the atmosphere correctly simulated? What is the impact of the urban canopy on onshore air temperature, wind speed and lake breezes? Also the diffusive processes (numerical and physical) might degrade the quality of the predicted lake breezes. These aspects should be subjects of the future studies.

Acknowledgment:

The authors would like to thank all the participants of the PanAm project including John MacPhee and Reno Sit. Special thanks to Ivan Heckman and Dr. Zhipeng Qu for their assistance with data analysis.

References:

Atkinson, B. W. (1981): Mesoscale Atmospheric Circulations. Academic Press, 495 pp.

Bélair, S., L. P. Crevier, J. Mailhot, B. Bilodeau, and Y. Delage (2003a): Operational implementation of the ISBA land surface scheme in the Canadian Regional Weather Forecast Model. Part I: Warm season results. *J. Hydrometeor*., 4, 352–370.

Bélair, S., R. Brown, J. Mailhot, B. Bilodeau, and L. P. Crevier (2003b): Operational implementation of the ISBA land surface scheme in the Canadian Regional Weather Forecast Model. Part II: Cold season results. *J. Hydrometeor*., 4, 371–386.

Biggs, W.G. and M.E. Graves (1962): A Lake Breeze Index. *J. Appl. Meteorol.* **1**:474- 480.

Boodoo, S., D. Hudak, N. Donaldson, and M. Leduc (2010): Application of Dual-Poliarization Radar Melting-Layer Detection Algorithm. J. of Appl. Met. and Clim., 49(8), 1779-1793.

Brasnett, B. (2008): The impact of satellite retrievals in a global seasurface-temperature analysis. *Quart. J. Roy. Meteor. Soc*., 134, 1745–1760.

Charnock, H. (1955): Wind stress over a water surface. *Quart. J. Roy. Meteor*. Soc., 81, 639–640

Comer, N. T. and I. G. McKendry (1993): Observations and numerical modelling of Lake Ontario breezes, *Atmos.-Ocean*, 31, 481-499.

Côté, J., S. Gravel, A. Méthot, A. Patoine, M.Roch, and A. Staniforth (1998): The operational CMC–MRB Global Environmental Multiscale (GEM) model. Part I: Design considerations and formulation. *Mon. Wea. Rev*., 126, 1373–1395.

Curry, M., J. Hanesiak, S. Kehler, D. Sills and N. Taylor (2016): Ground-based Observations of the Thermodynamic and dynamic properties of lake-breezes in southern Manitoba, Canada. *Boundary Layer Meteorol*.

Darby, L. S., W. D. Neff, and R. M. Banta (1999): Multiscale analysis of a meso-b frontal passage in the complex terrain of the Colorado Front Range. *Mon. Wea. Rev*., 127, 2062-2081.

Deacu, D., V. Fortin, E. Klyszejko, C. Spence, and P. D. Blanken (2012): Predicting the net basin supply to the Great Lakes with a hydrometeorological model. *J. Hydrometeor*., 13, 1739–1759.

DiCiccio, T.J. and B. Efron, (1996): Bootstrap confidence intervals (with discussion), *Statistical Science*, 11, 189–228.

Dupont, F., Chittibabu, P., Fortin, V., Rao, Y. R., and Lu, Y.: Assessment of a NEMO-based hydrodynamic modelling system for the Great Lakes (2012): *Water Qual. Res. J. Can*., 47, 198–214.

Estoque, M.A., J. Gross and H.W. Lai (1976): A Lake Breeze over Southern Lake Ontario. *Mon. Wea. Rev.* 104, 386-396.

Estoque, M.A. and J.M. Gross (1981): Further Studies of a Lake Breeze Part II: Theoretical Study. *Mon. Wea. Rev.* 109, 619-634.

Fillion L, Tanguay M, Lapalme E, Denis B, Desgagne M, Lee V, Ek N, Liu Z, Lajoie M, Caron J-F, Pag´e C. (2010): The Canadian regional data assimilation and forecasting system. *Weather and Forecasting*, 25, 1645-1669.

Girard, C., A. Plante, M. Desgagné, R. McTaggart-Cowan, J. Côté, M. Charron, S. Gravel, V. Lee, A. Patoine, A. Qaddouri, M. Roch, L. Spacek, M. Tanguay, P.A. Vaillancourt, and A. Zadra, (2014): Staggered Vertical Discretization of the Canadian Environmental Multiscale (GEM) Model Using a Coordinate of the Log-Hydrostatic-Pressure Type. *Mon.Wea.Rev*, 142, 1183-1196.

Hanna, S. R. (1994): Mesoscale meteorological model evaluation techniques with emphasis on needs of air quality models. *Mesoscale Modeling of the Atmosphere, Meteor. Monogr.*, No. 47, Amer. Meteor. Soc., 47–62.

Harris, L. and V. R. Kotamarthi (2005): The characteristics of the Chicago Lake breeze and its effects on trace particle transport: results from an episodic event simulation. *J Appl Meteorol* 44, 1637–1654

Hastie, D. R., J. Narayan, C. Schiller, H. Niki, P. B. Shepson, D. M. L. Sills, P. A. Taylor, Wm. J. Moroz, J. W. Drummond, N. Reid, R. Taylor, P. B. Roussel and O. T. Melo (1999): Observational evidence for the impact of lake breeze circulation on ozone concentrations in southern Ontario. *Atmospheric Environment*, 33, 323-335

Hayden, K.L., D.M.L. Sills, J.R. Brook, S.M. Li, P.A. Makar, M.Z. Markovic, P. Liu, K.G. Anlauf, J.M. O'Brien, Q. Li and R. McLaren (2011): Aircraft study of the impact oflake-breeze circulations on trace gases and particles during BAQS-Met 2007. *Atmos. Chem. Phys*. 11, 10173e10192.

Hudak, D., P. Rodriguez, G. Lee, A. Ryzhkov, F. Fabry, and N. Donaldson (2006): Winter precipitation studies with a dual polarized C-band radar. Preprints, Fourth European

Conf. on Radar in Meteorology and hydrology (ERAD 2006), Barcelona, Spain, Servei Meteorologic de Catalunya, 9-12.

Joe, P., S. Bélair, N.B. Bernier, J.R. Brook, D. Brunet, V. Bouchet, W. Burrows, J.P. Charland, A. Dehghan, N. Driedger, C. Duhaime, G. Evans, R. Frenette, I. Gultepe, D. Henderson, A. Herdt, N. Hilker, L. Huang, E. Hung, G. Isaac, D. Johnston, C.-H. Jeong, J. Klaassen, S. Leroyer, H. Lin, M. MacDonald, J. MacPhee, Z. Mariani, J. Reid, A. Robichaud, Y. Rochon, D. Sills, K. Shairsingh, C. Stroud, Y. Su, N. Taylor, J.M. Wang, J. Vanos, J. Voogt, T. Wiechers, S. Wren, H. Yang, and T. Yip (2017): The Pan-American Games Science Showcase Project. *Amer. Meteor. Soc*., submitted January 2017.

Keen, C.S. and W.A. Lyons, (1978): Lake/Land Breeze Circulations on the Western Shore of Lake Michigan. *J. Appl. Meteorol.* 17, 1843-1855.

Kehler, S., J. Hanesiak, M. Curry, D. Sills and N. Taylor, (2016): High resolution Deterministic Prediction System (HRDPS) simulations of Manitoba lake breezes, *Atmos. Ocean.*54, 93-107.

King, P. W. S., M. Leduc, D. M. L. Sills, N. R. Donaldson, D. R. Hudak, P. I. Joe, and B. P. Murphy (2003): Lake breezes in Southern Ontario and their relation to tornado climatology. *Weather and Forecasting*, 18, 795-807.

Leroyer, S., S. Bélair, J. Mailhot, and I. Strachan, (2011): Microscale numerical prediction over Montreal with the Canadian external urban modeling system. J. Appl. Meteor. Climatol., 50, 2410–2428.

Leroyer, S., S. Bélair, S.Z. Husain and J. Mailhot, Subkilometer Numerical Weather Prediction in an Urban Coastal Area: A Case Study over the Vancouver Metropolitan Area, (2014): Subkilometer Numerical Weather Prediction in an Urban Coastal Area: A Case Study over the Vancouver Metropolitan Area, *J. Appl. Meteorol. Clim.*, 53, 1433-1453.

Lyons, W.A. (1972): The Climatology and Prediction of the Chicago Lake Breeze. *J. Appl. Meteorol.*, 11, 1259-1270.

Mariani, Z., A. Dehghan, P. Joe, D. Sills (2017): Observations of lake breeze events during the Toronto 2015 Pan/Parapan American Games. *Boundary Layer Meteorol.*, Accepted in June 2017.

Mason, P. J., and A. R. Brown (1999): On subgrid models and filter operations in large eddy simulations. *J.Atmos. Sci.*, 56, 2101–2114,

Milbrandt, J. A., and M. K. Yau (2005): A multimoment bulk microphysics parameterization. Part I: Analysis of the role of the spectral shape parameter. *J. Atmos. Sci.*, 62, 3051–3064

Noilhan, J., and S. Planton (1989): A simple parameterization of land surface processes for meteorological models. *Mon. Wea. Rev.*, 117, 536–549.

Pielke, R. A. (1984): Mesoscale Meteorological Modeling. Academic Press, 612 pp.

Sills, D., P. Taylor, P. King, W. Hocking and I. Nichols (2002): ELBOW 2001 - studying the relationship between lake breezes and severe weather: project overview and preliminary results. *Preprints, 21st Severe Local Storms Conference*, San Antonio, TX, *Amer. Meteorol. Soc.*, 611-614.

Sills, D. M. L., J. R. Brook, I. Levy, P. A. Makar, J. Zhang, and P. A. Taylor (2011): Lake breezes in the southern Great Lakes region and their influence during BAQS-Met 2007. *Atmos. Chem. Phys.*, 11, 7955-7973.

Tsunematsu, N., H. Iwai, S. Ishii, Y. Murayama, M. Yasui, and K. Mizutani (2009): The Formation of Sharp Multi-Layered Wind Structure over Tokyo Associated with Sea-breeze Circulation. SOLA, 5, 1-4.

Wentworth, G.R., J.G. Murphy, and D.M.L. Sills (2015): Impact of lake breezes on ozone and nitrogen oxides in the Greater Toronto Area. *Atmos. Env*., 109, 52-60.

Zadra, A., D. Caya, J. Cote, B. Dugas, C. Jones, R. Laprise, K. Winger, and L.-P. Caron (2008): The next Canadian regional climate model. *Phys. Canada*, 64, 75–83.

Table 1. Selected surface stations.

Surface sites	Latitude	Longitude	Type	Height of sensors from ground (m)
Z2D	43°38'22.3"N	79°20'53.7"W	Compact/ground	2.5
L1B	43°40'41.5"N	79°26'34.6"W	Compact/rooftop	10.3
L1C	43°41'56.2"N	79°27'5.7"W	Compact/rooftop	9.1
L1D	43°43'7.1"N	79°28'7.4"W	Compact/rooftop	4
L1E	43°44'51.8"N	79°28'47.6"W	Compact/rooftop	9.1
L1F	43°49'3.2"N	79°31'24.2"W	Compact/rooftop	7.3
A2T	43°51'47.7"N	79°32'28.9"W	Tower/ground	10 (wind) 1.5 (temperature and dew point)

Table 2. RDPS and GEM configurations.

Domains	RDPS	Domain 1 (nested)	Domain 2 (nested)	Domain 3 (nested)
Horizontal grid spacing (km)	10	2.5	1	0.25
Number of grid points	360×256	512x512	512x512	1024×1024
Vertical momentum levels	58	57	57	57
Levels below 500 m	6	15	15	15
Levels below 1500 m	13	26	26	26
Time steps (s)	450	60	30	12
Land surface model (URB)	ISBA	ISBA	ISBA+TEB	ISBA+TEB
Land surface model (VEG)	ISBA	ISBA	ISBA	ISBA
Planetary Boundary Layer	MoisTKE	MoisTKE	MoisTKE	MoisTKE
Microphysics	ConSun	MY-DM	MY-DM	MY-DM

Table 3. Temperature drops, T, dew point rises, Td, and wind shift timings due to lake-breeze front at selected surface stations. The n/a for Td means highly variable measurements. Also when the wind shift to onshore was not observed, n/a was recoreded for the timing. Zero means no decrease in temperature (or increase in dew point) was occurred.

		observations			GEM 2.5 km			GEM 1 km			GEM 0.25 km		
Day	Station	T↓ (˚C)	Td↑ (˚C)	Time (UTC)	T↓ (˚C)	Td↑ (˚C)	Time (UTC)	T↓ (˚C)	Td↑ (˚C)	Time (UTC)	T↓ (˚C)	Td↑ (˚C)	Time (UTC)
Jul15	Z2D	1.3	1.6	15:08	0.9	0	16:30	0.7	0.7	16:15	0	0.6	16:15
Jul15	L1B	2.3	3	18:45	0	3	n/a	0	0.6	n/a	0.4	1.6	n/a
Aug9	Z2D	1.4	1.1	14:42	0.2	0.3	16:15	0	0.3	16:00	0	0.3	16:00
Aug9	L1B	1.1	n/a	14:40	0	0	14:45	0.1	0	14:45	0.2	0.9	14:45
Aug9	L1C	1.1	n/a	15:10	0	0	14:45	0.2	0	15:30	0.2	1	15:15
Aug9	L1D	1.6	1.3	15:48	0	0	15:15	0.5	0.8	15:45	0	1	15:15
Aug9	L1E	1.2	n/a	16:30	0	0	14:15	0.2	0.9	16:15	0.4	0.7	15:00
Aug9	L1F	1.5	2.1	16:43	0	0	14:45	0.2	0.4	16:00	0.3	1	16:15
Aug9	A2T	2.5	n/a	17:38	0	0.2	16:45	0	0.9	17:00	0	2.5	16:00

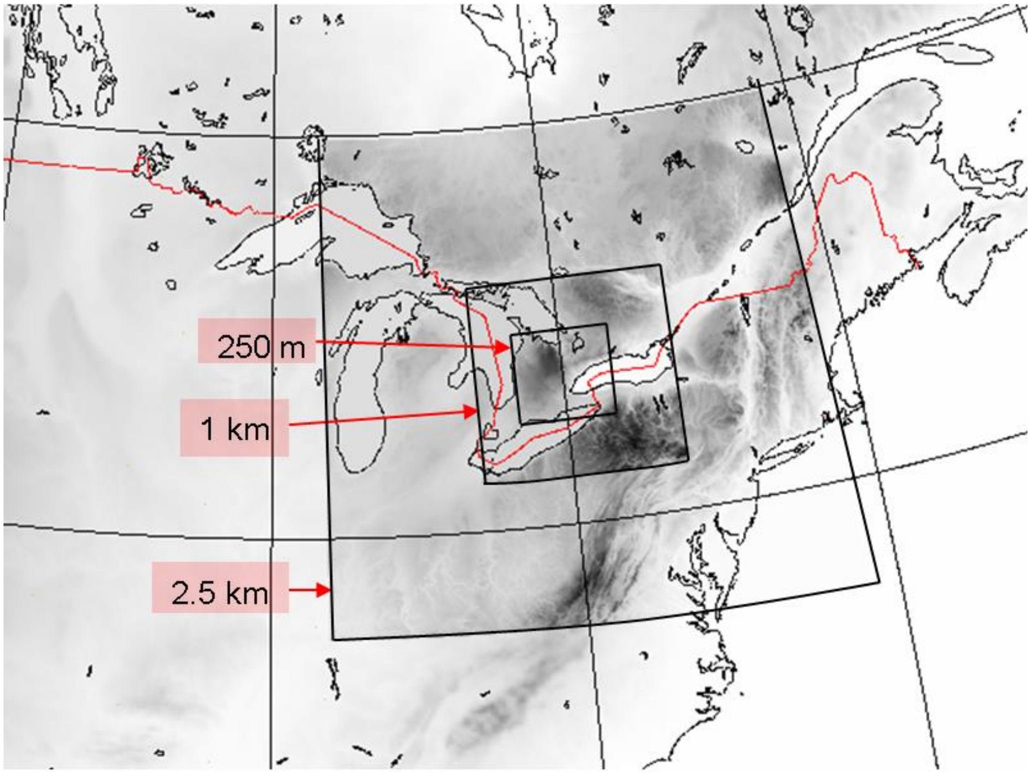

Fig. 1. The GEM domains

(a)

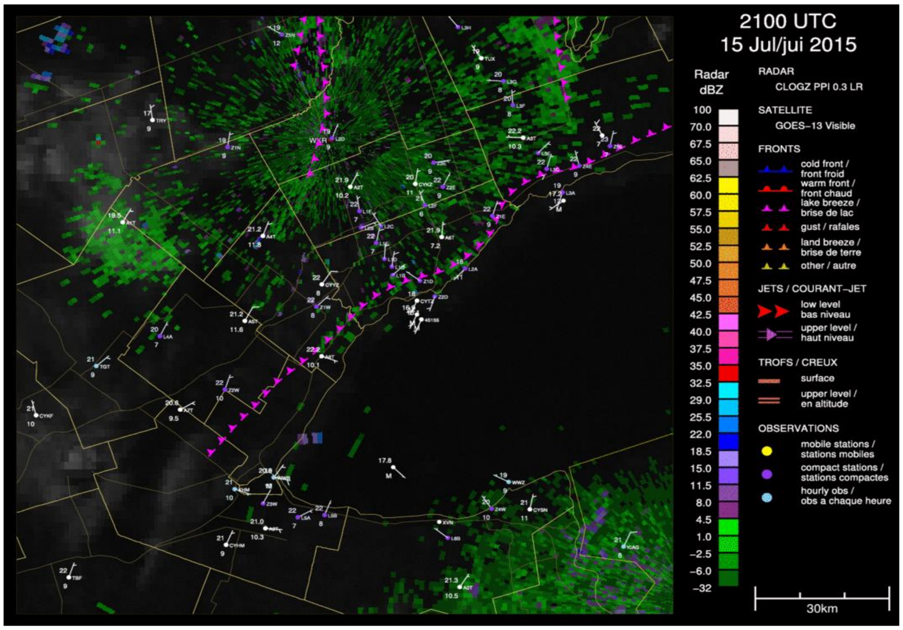

(b)

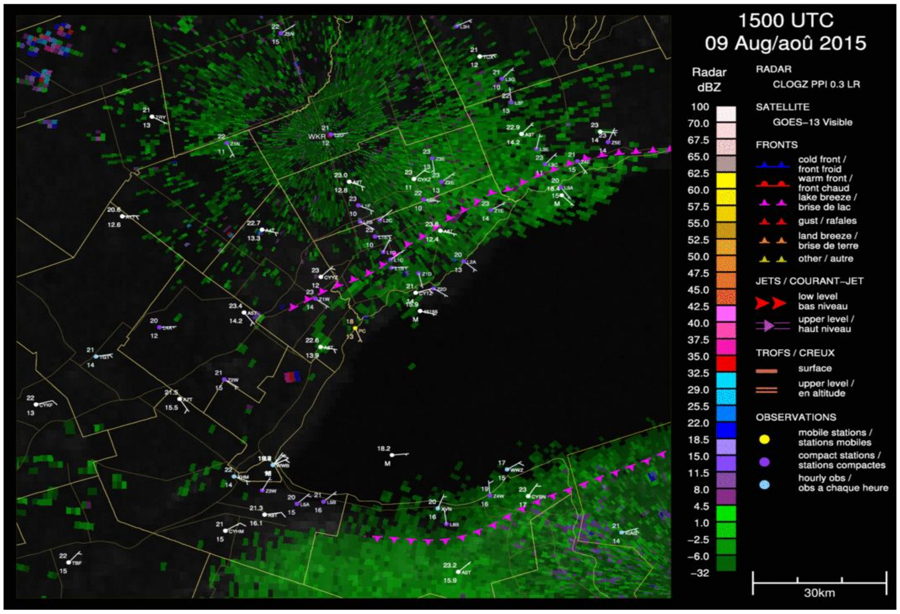

Fig. 2. Mesonet analyses (a) on July 15 at 21:00 UTC, (b) on August 9 at 15:00 UTC. The meteorological data including wind barbs and the radar reflectivity are shown. The locations of lake-breeze fronts are indicated by the magenta lines. Note that the lake-breeze fronts at the top of the Fig. 2a are generated by Lake Simcoe and Georgian Bay.

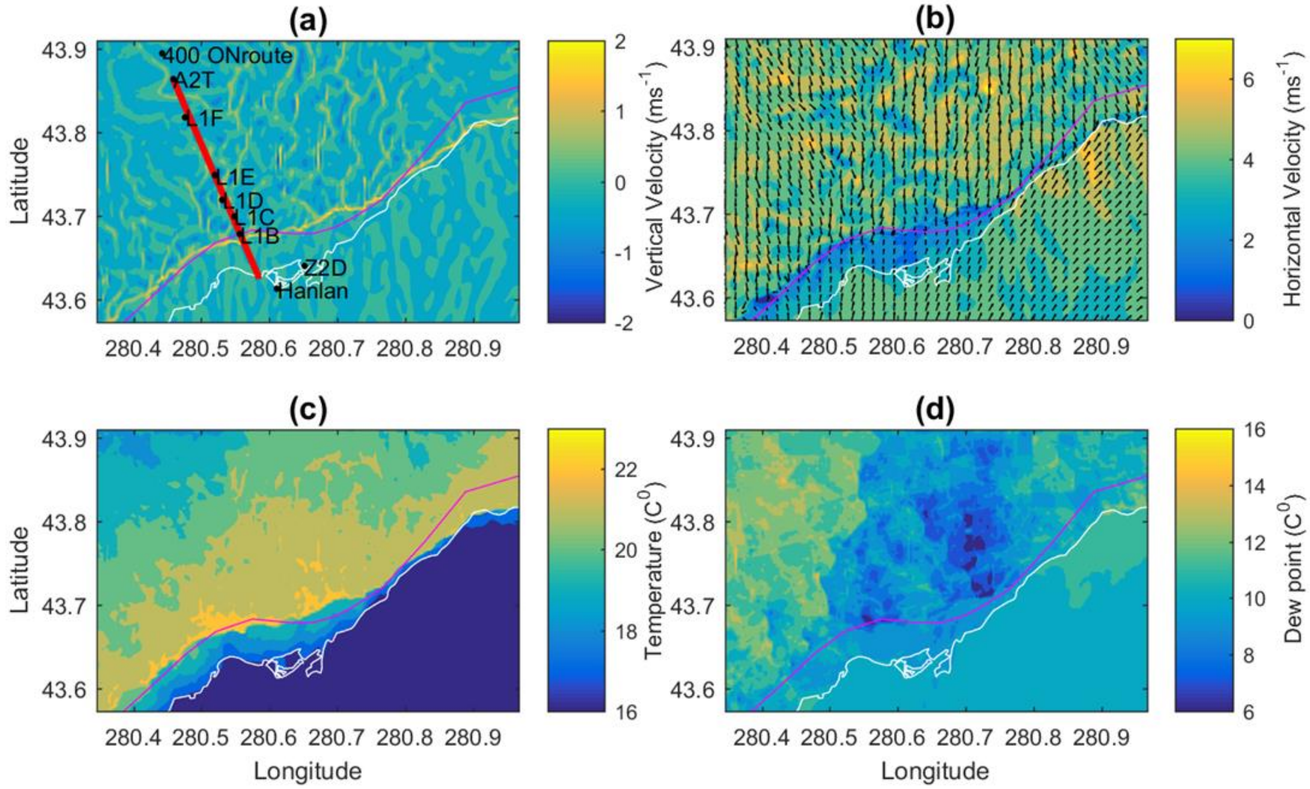

Fig. 3. The GEM 0.25 km numerical output for the lake-breeze event of July 15 at 21:00 UTC, 2015. Plots of (a) vertical velocity (ms^{-1}) at 120 m AGL, (b) horizontal wind speed (ms^{-1}) and direction ($^{\circ}$) at 10 m AGL and (c) temperature (C$^{\circ}$) and (d) dew point (C$^{\circ}$) at 5 m AGL. The plots cover an area of ~50×30 km^2. The white and magenta lines represent the GTA lakeshores and the lake-breeze front determined by the mesoscale analyses, respectively. The red line indicates the cross-section passing through the selected surface stations in Table 2. Hanlan's Point and Highway 400 ONroute are the locations of the lidars, and Z2D is the location of the surface station at the lakeshore.

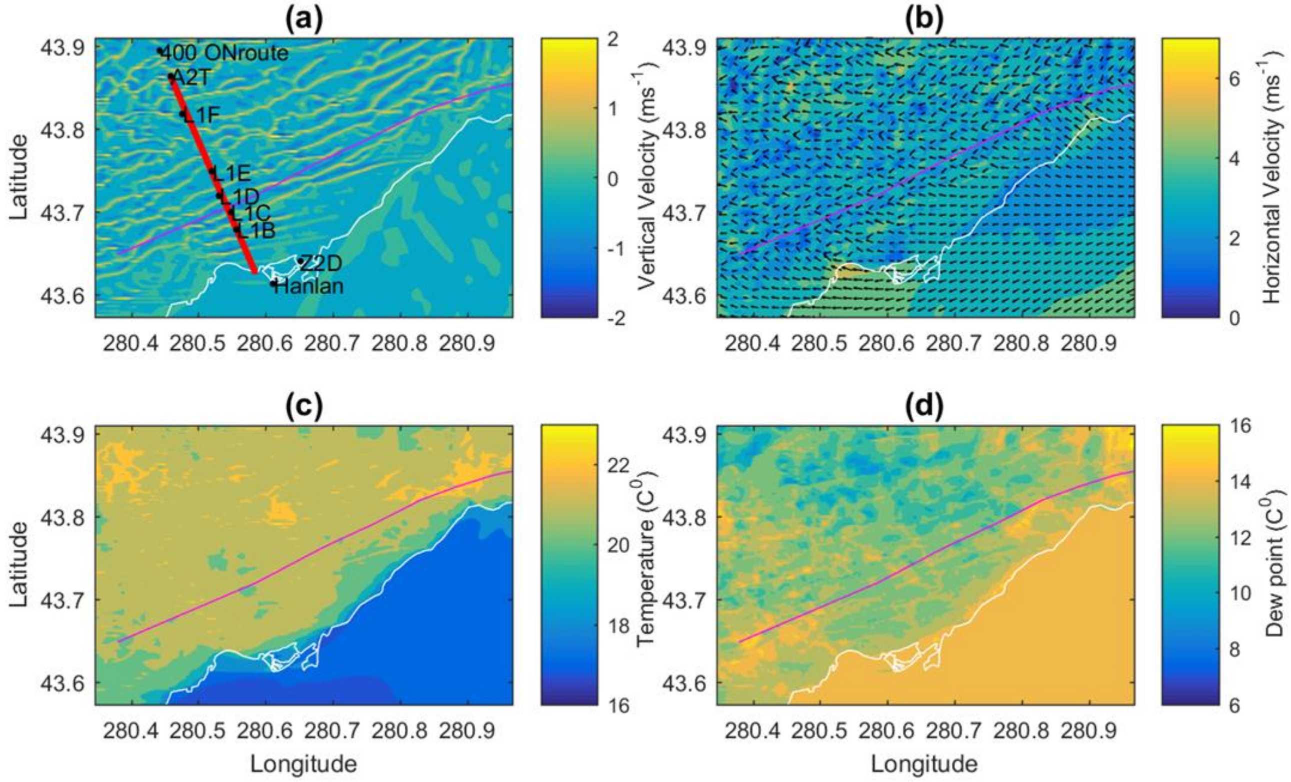

Fig. 4. Same as Fig. 3, except for August 9, 2015 at 15 UTC.

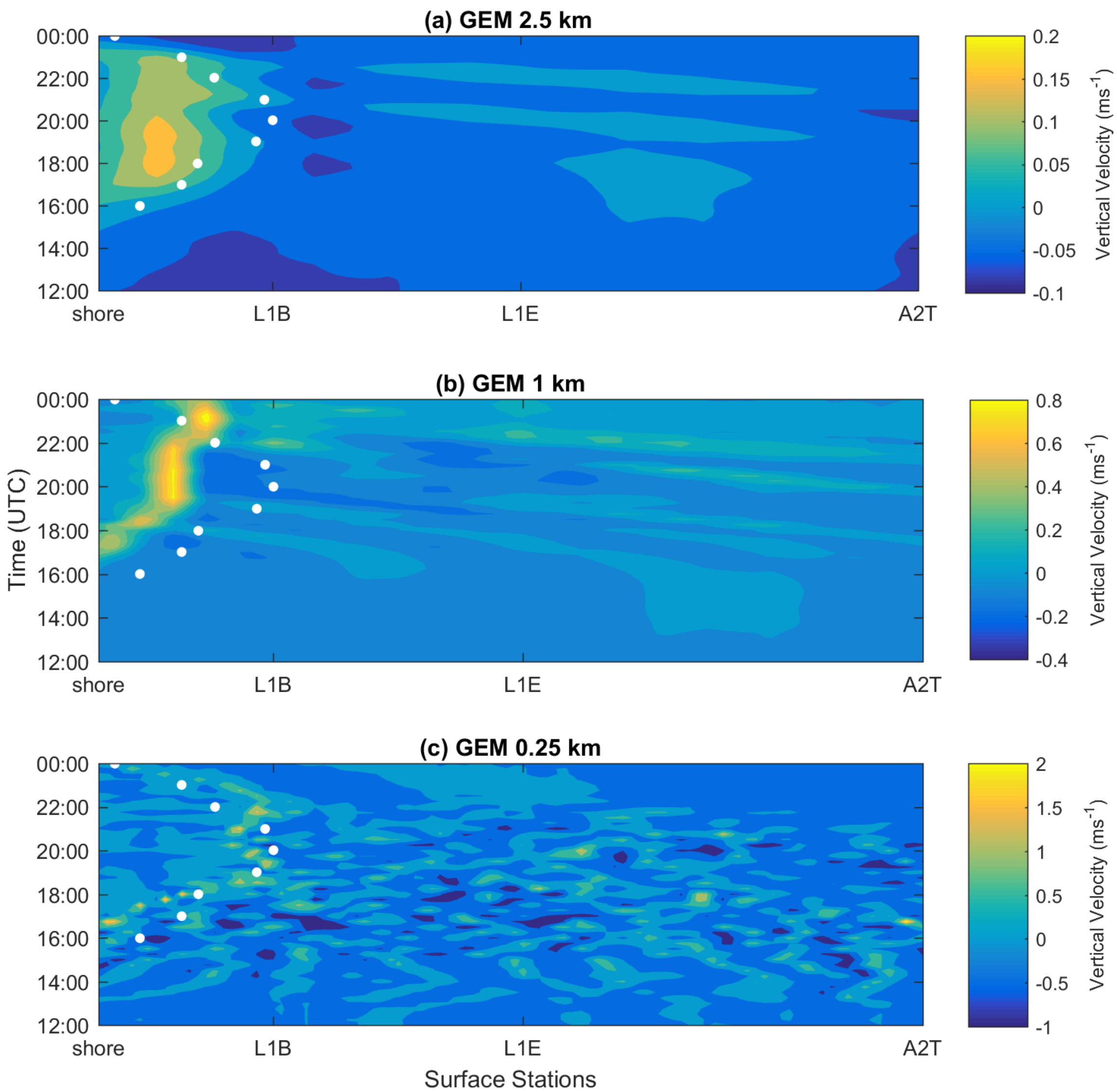

Fig. 5. vertical velocity (ms^{-1}) along the shore-A2T cross-section at 120 m AGL for (a) GEM 2.5 km, (b) GEM 1 km and (c) GEM 0.25 km on July 15. The location of the cross-section in the GTA is shown in Fig. 3a. Note that figures are plotted using different scales to clearly show the updraft zone.

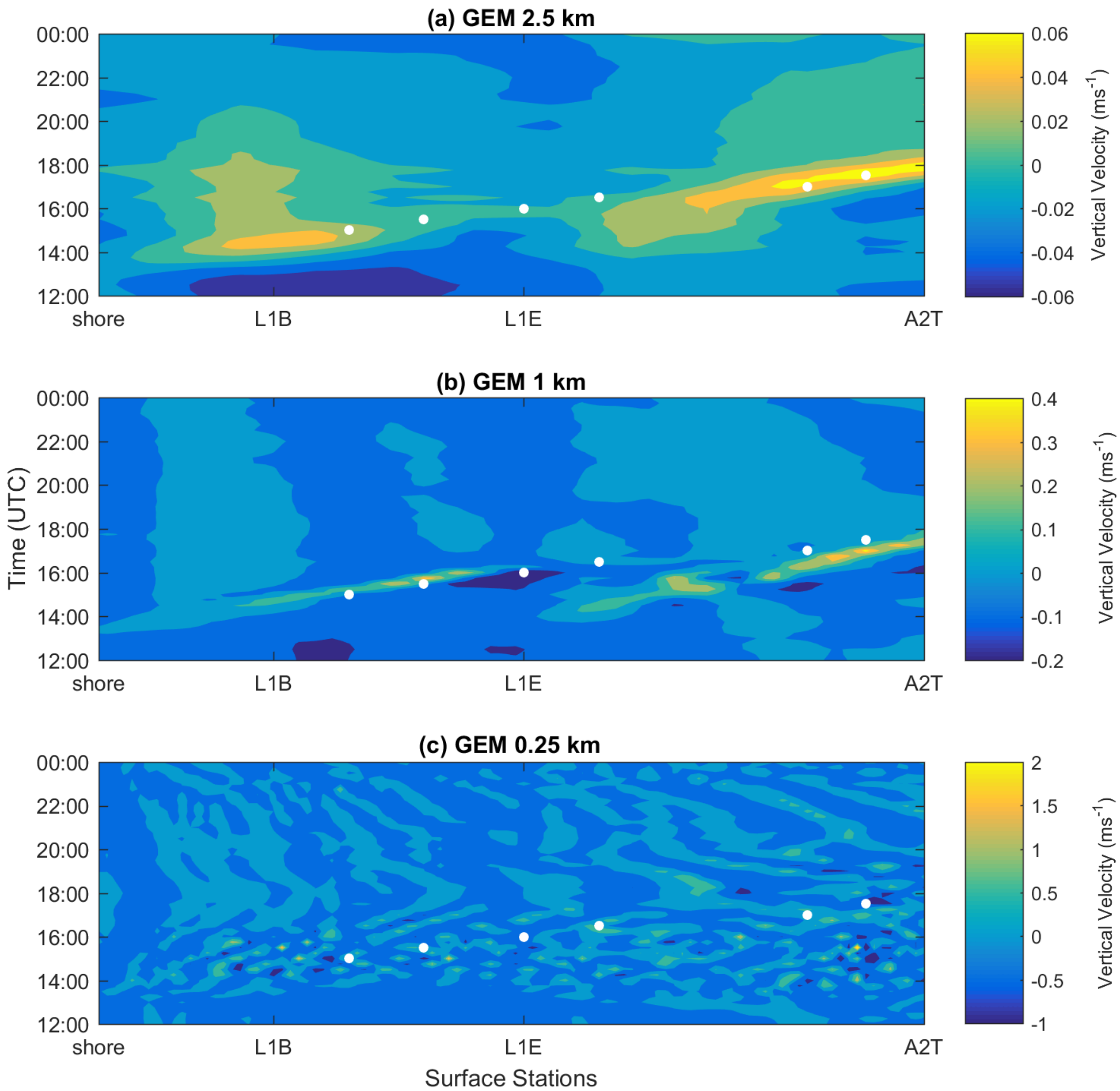

Fig. 6. The same as Fig. 5, except for August 9, 2015

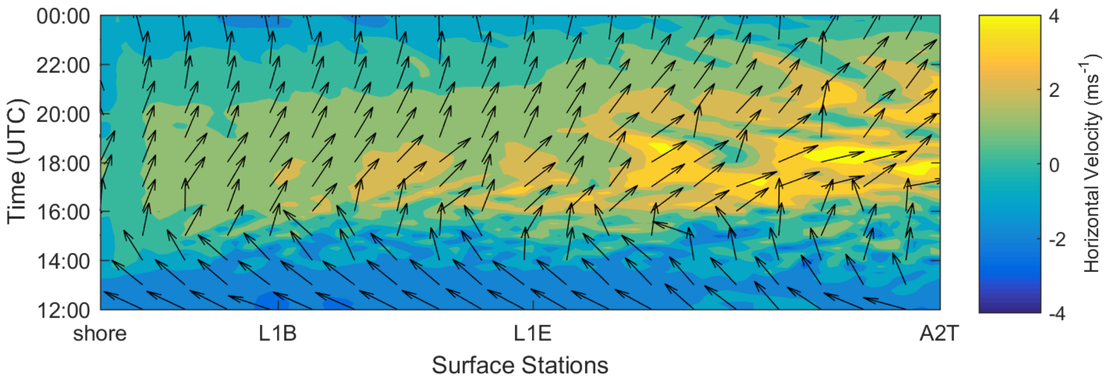

Fig. 7. Horizontal velocity (ms^{-1}) along the shore-A2T cross-section for GEM 0.25 km on August 9. North is on the right.

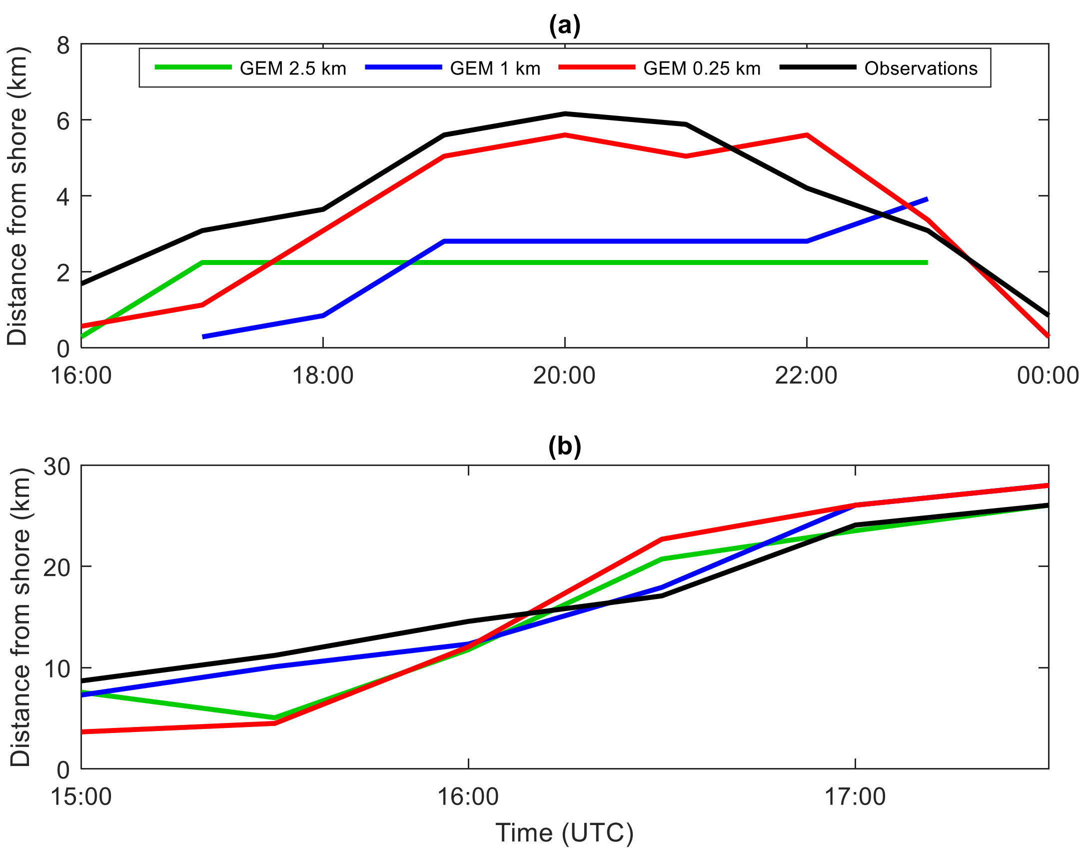

Fig. 8. Locations of the modeled vertical velocity maxima and observed lake-breeze front along the shore-A2T cross-section (red line in Figs. 3a and 4a) on (a) July 15 and (b) August 9.

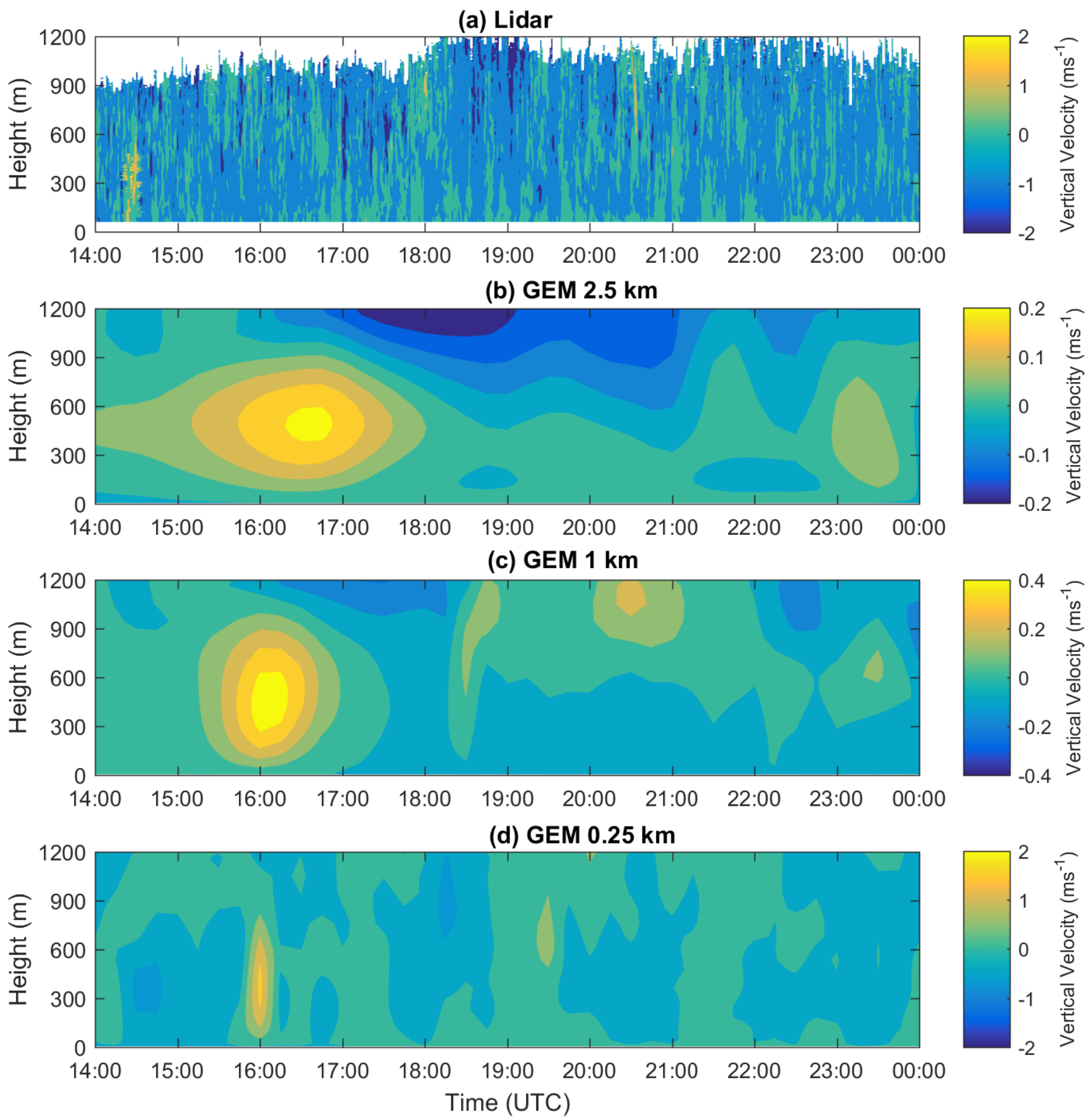

Fig. 9. Vertical velocity in ms^{-1} (a) measured by lidar at Hanlan's Point from 14:00 UTC on July 15 until 00:00 UTC on July 16, and the predicted vertical velocities (ms^{-1}) at the nearest grid point to Hanlan's Point for the same period with (b) GEM 2.5 km. (c) GEM 1 km and (d) GEM 0.25 km. The white color indicates no measurements. Note that figures are plotted using different scales to clearly show the updraft zone, however the scales for (a) and (d) are the same.

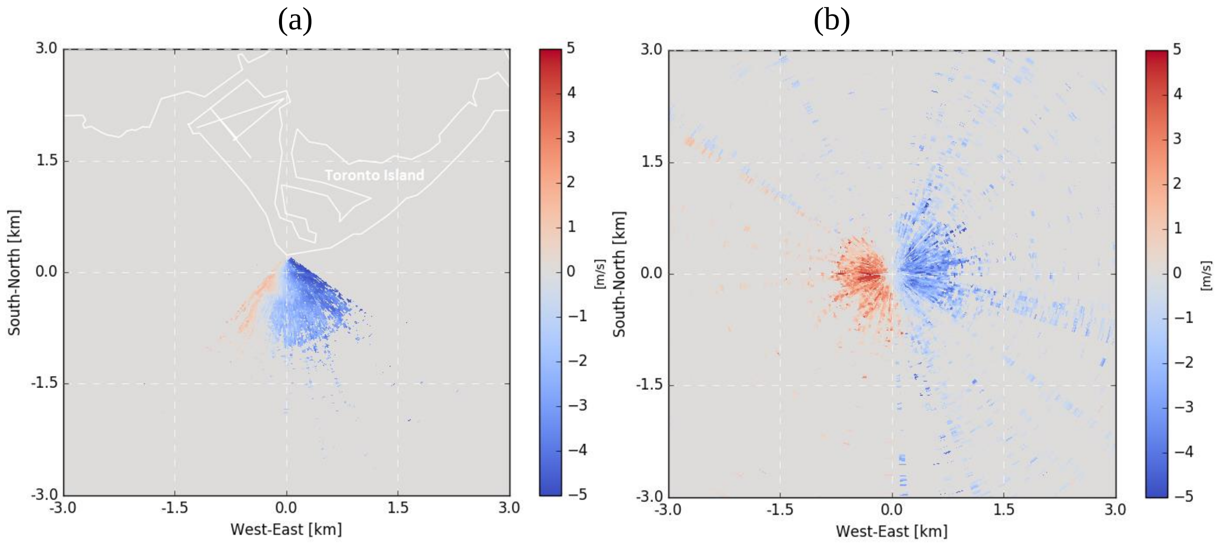

Fig. 10. Lidar measurements of radial velocity in ms^{-1} (PPI) at (a) Hanlan's Point on July 15 at 14:24 UTC and (b) Highway 400 ONroute on August 9 at 18:14 UTC. Negative (blue) velocities represent winds towards the lidar (onshore); positive (red) velocities represent winds away from the lidar (offshore).

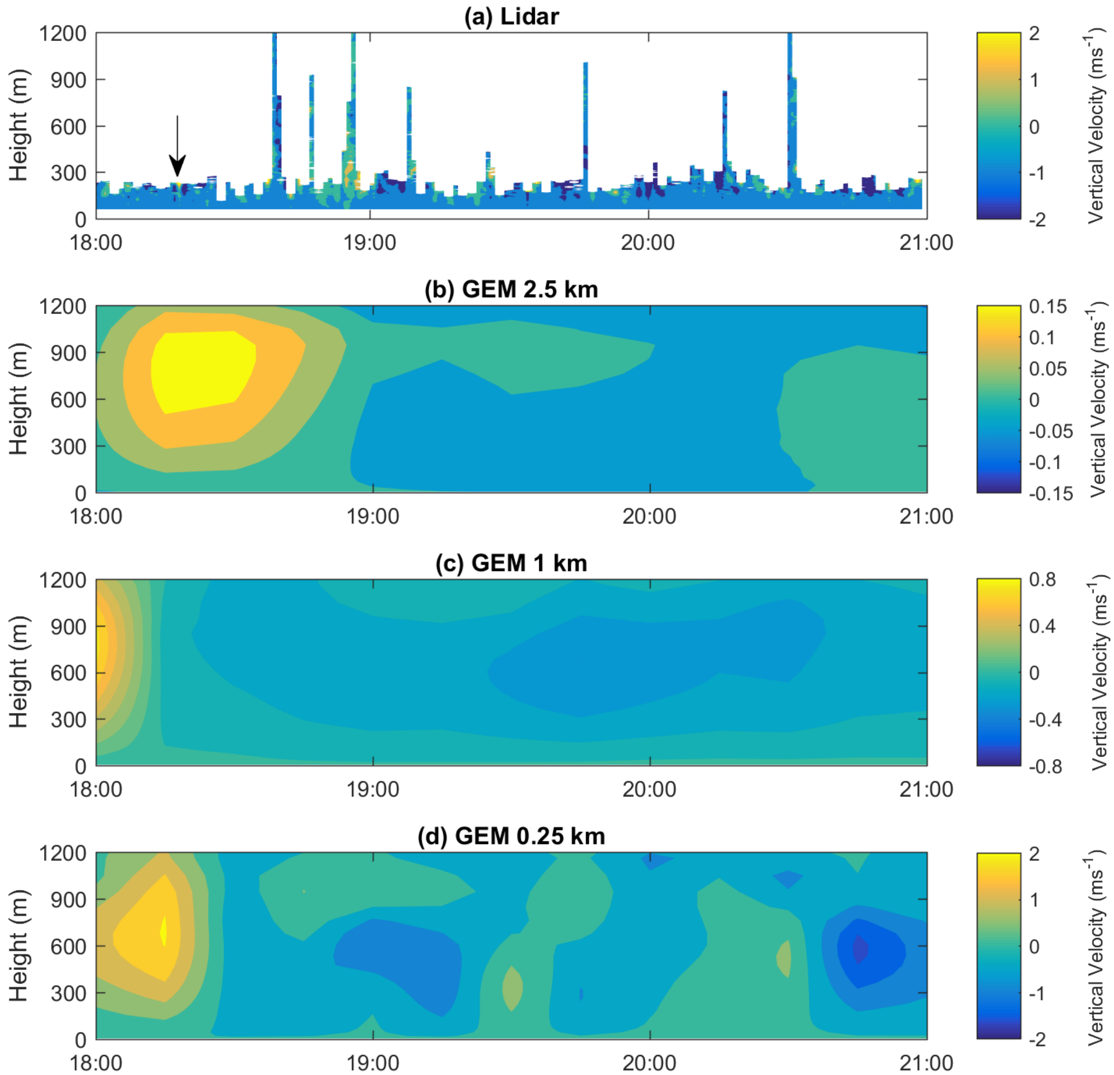

Fig. 11. The same as Fig. 9 except at Highway 400 ONroute from 18:00 UTC until 21:00 UTC on August 9. The arrow shows the time and the location of the maximum vertical velocity for the available lidar measurements.

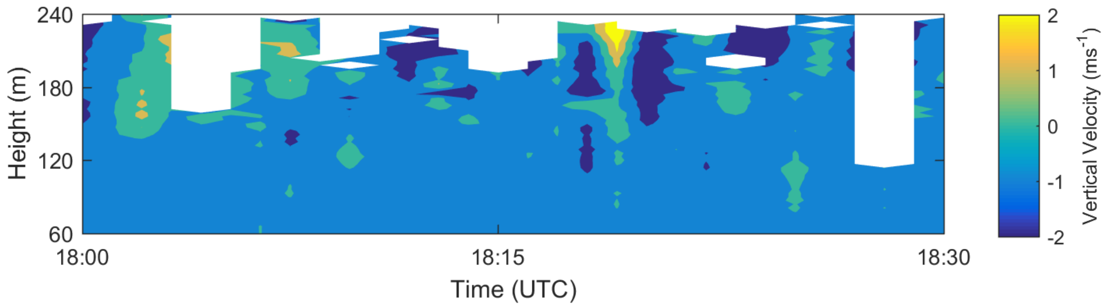

Fig. 12. Lidar measurements of vertical velocity from 18:00 UTC to 18:30 UTC at the height range from 60 to 240 m at Highway 400 ONroute. The maximum vertical velocity occurred at 18:19 UTC for the measurements below 240 m.

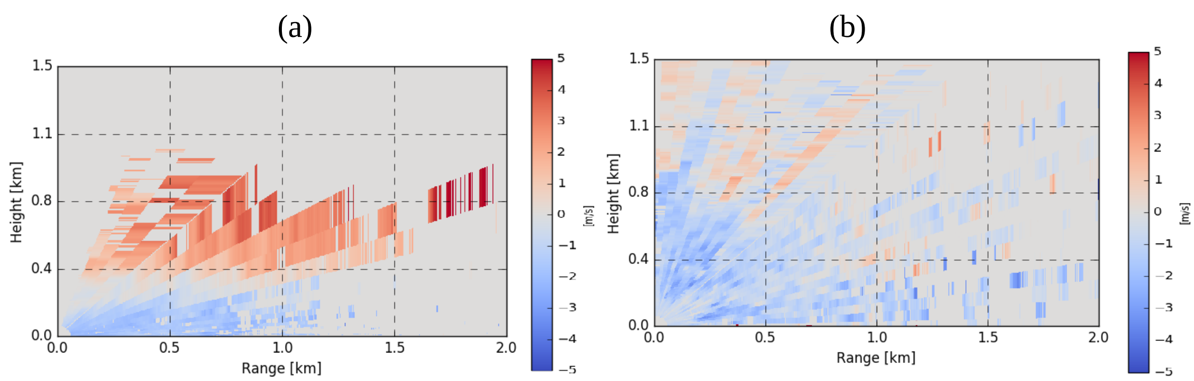

Fig. 13. Lidar measurements of radial velocity in ms^{-1} (RHI) at (a) Hanlan's Point on July 15 at 14:45 UTC (b) Highway 400 ONroute on August 9 at 18:15 UTC. Negative (blue) velocities represent winds towards the lidar; positive (red) velocities represent winds away from the lidar.The direction of radial velocity changed from onshore (blue) to offshore (red) at 190 m and 900 m at Hanlan's point and Highway 400 ONroute, respectively.

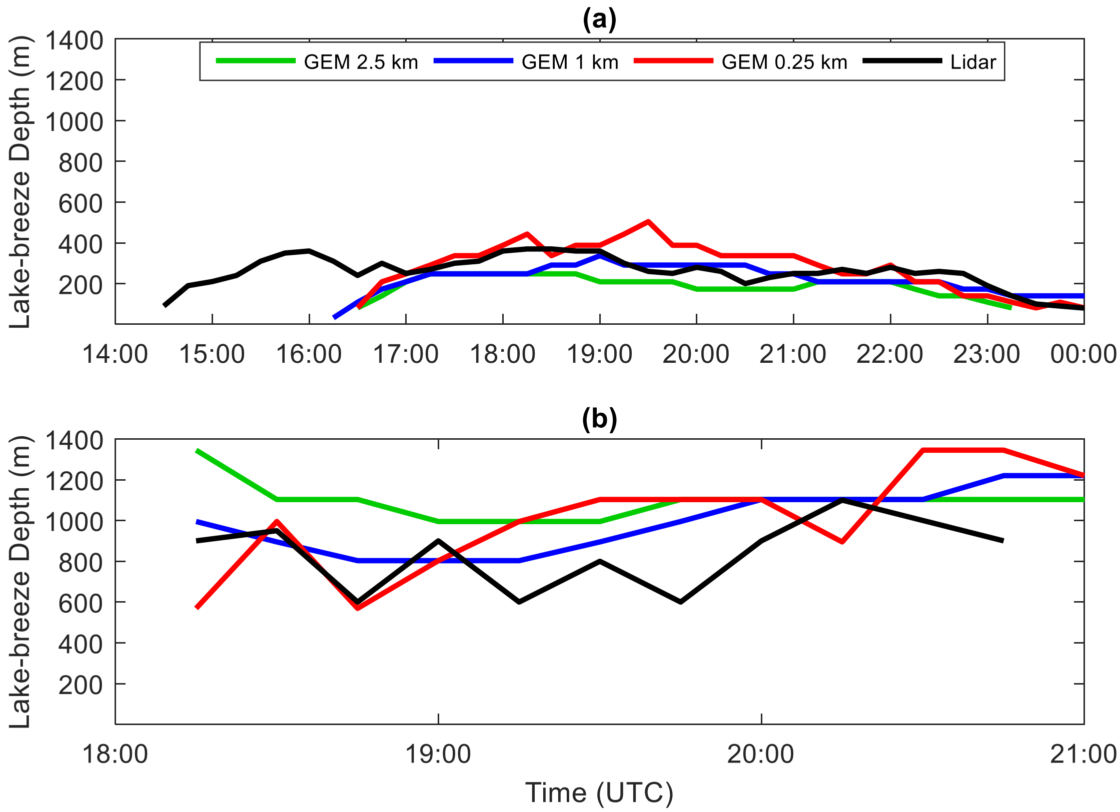

Fig. 14. Observed and predicted Lake-breeze depths using lidar and GEM at intervals of 15 minutes at (a) Hanlan's Point on July 15 and (b) Highway 400 ONroute on August 9. Note that the Lake-breeze front arrived at Hanlan's Point and Highway 400 ONroute approximately at 14:24 UTC and 18:15 UTC, respectively. Also the modeled depths were estimated at the nearest grid point to the lidar sites.

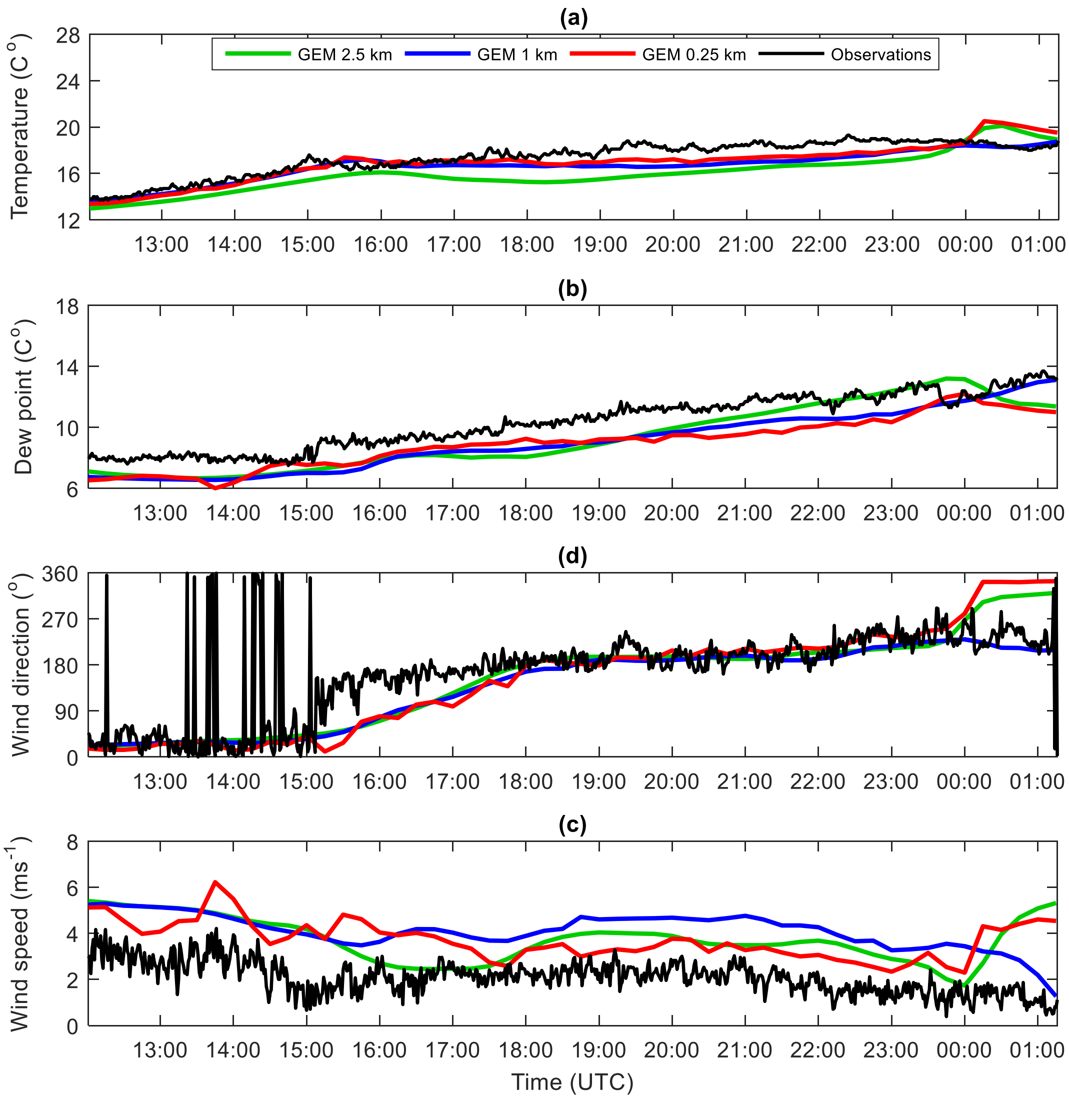

Fig. 15. Comparisons of observations with the model output at nearest grid point to Z2D station from the period of 12:00 UTC on July 15 to 01:15 UTC on July 16, 2015. (a) temperature (C$^{\circ}$), (b) dew point (C$^{\circ}$), (c) horizontal wind direction ($^{\circ}$) and (d) horizontal wind speed (ms^{-1}). The observed lake-breeze front arrived at 15:08 UTC. The temporal resolution of observations and predictions are 1 and 15 minutes, respectively.

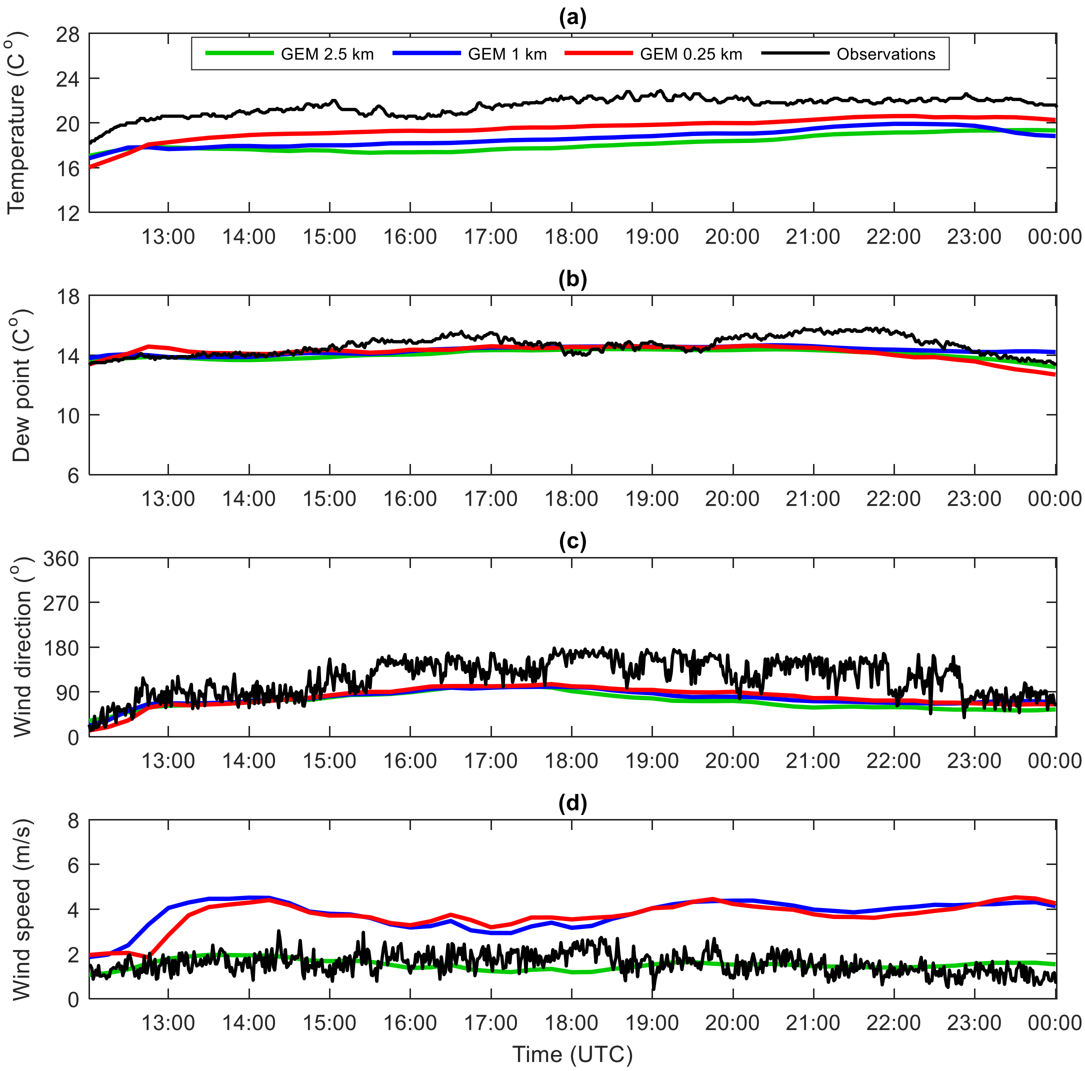

Fig. 16. The same as Fig.14 except from 12:00 UTC on August 9 to 00:00 UTC on August 10. The lake-breeze front arrived at 14:42 UTC.

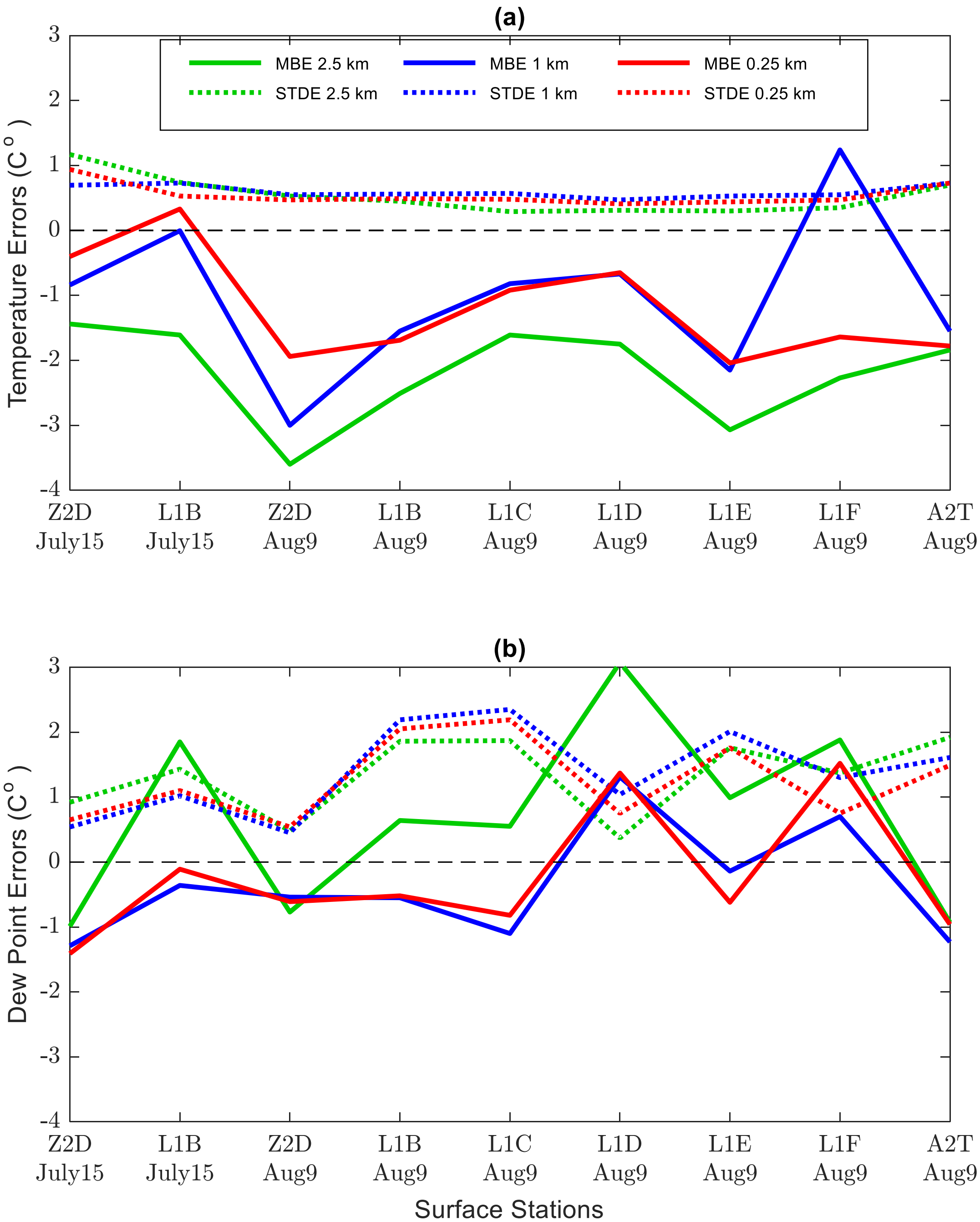

Fig. 17. The MBE and STDE values for (a) temperature (C°) and (b) dew point (C°) at the nearest grid point to surface stations for the periods of time that surface stations were affected by the lake-breeze circulations on July 15 and August 9.

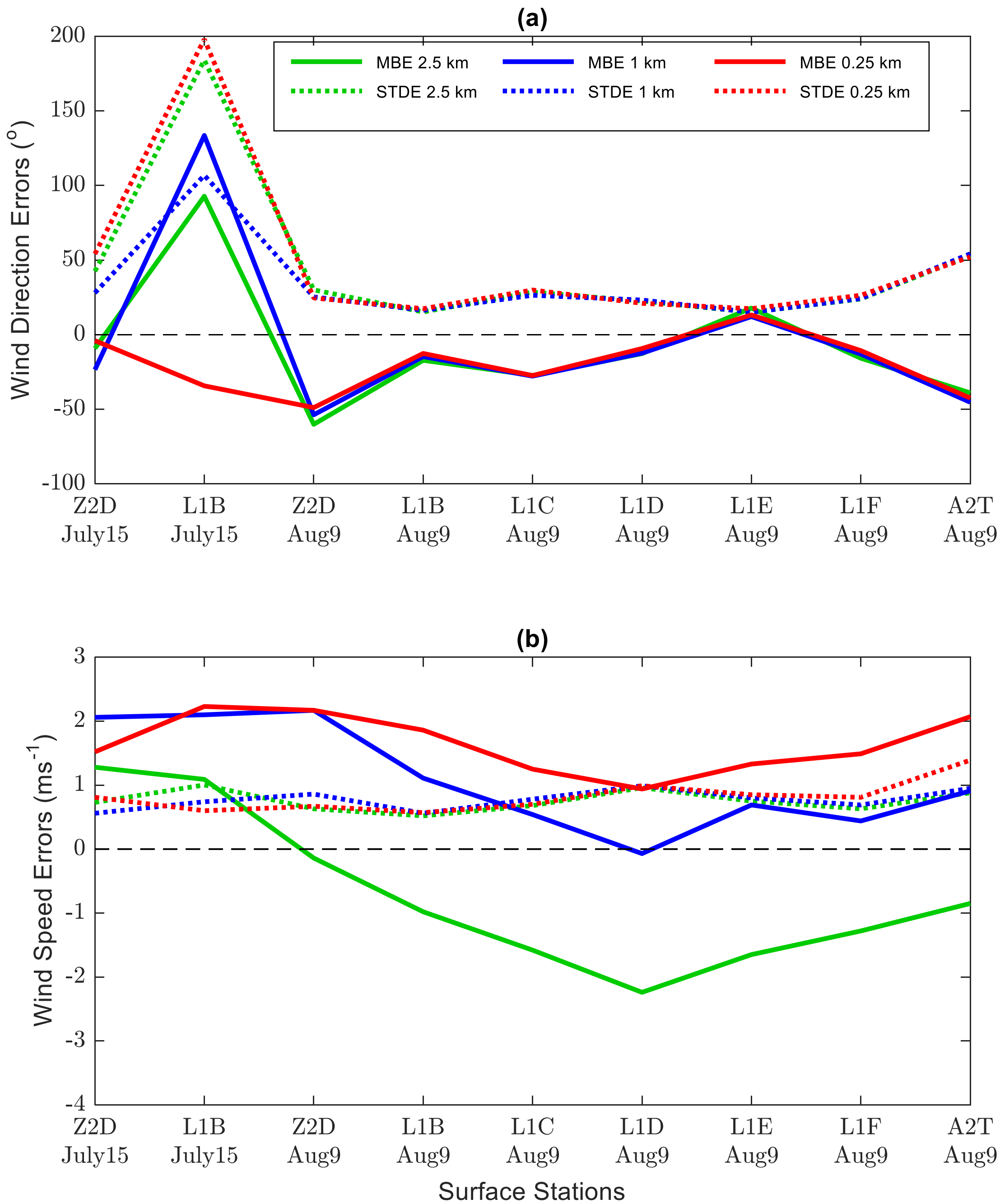

Fig. 18. The same as Fig. 17 except for (a) wind direction (°) and (b) wind speed (ms^{-1}).

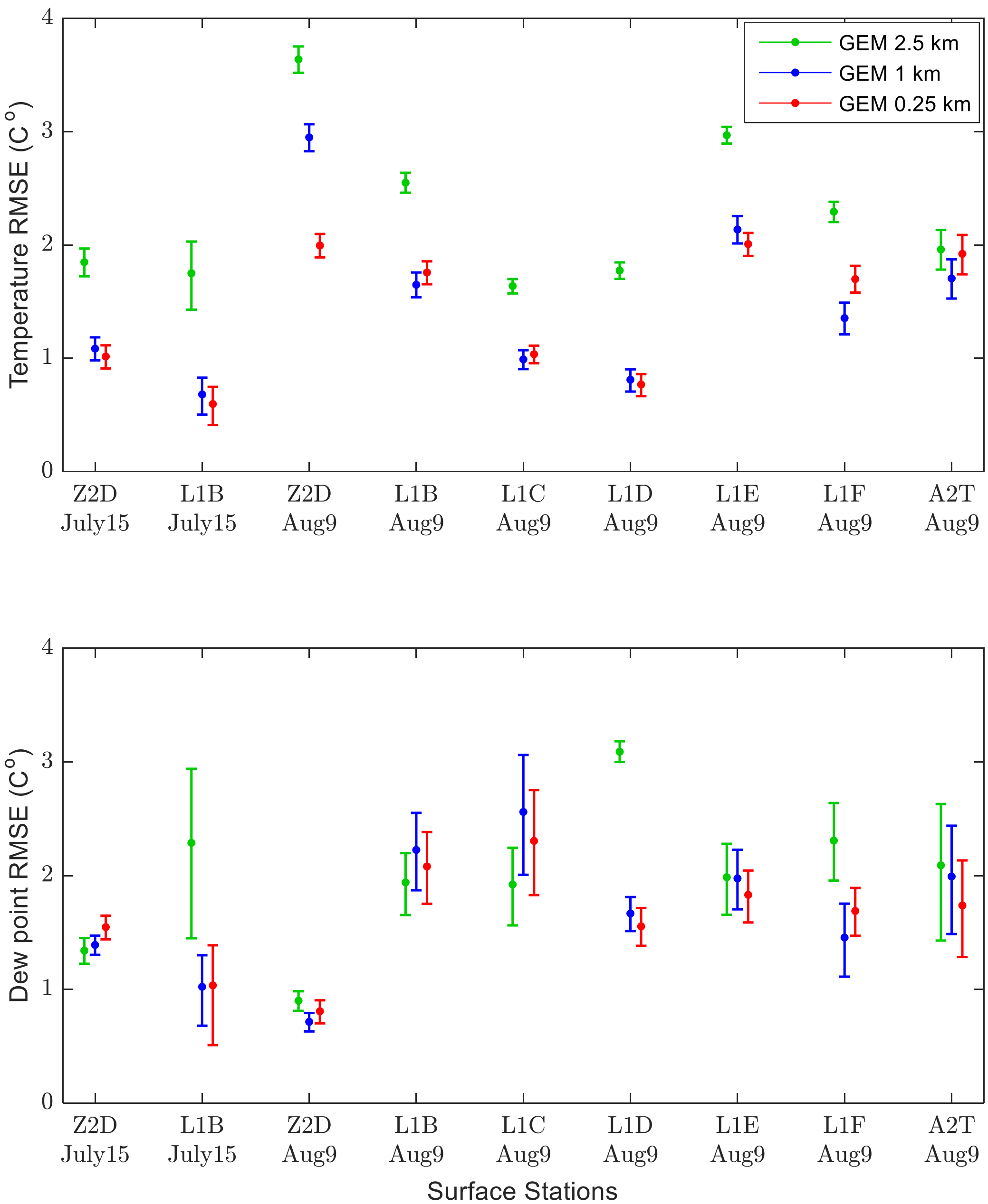

Fig. 19. The RMSE values and corresponding 10% and 90% confidence intervals for (a) temperature (C°) and (b) dew point (C°) at the nearest grid point to surface stations for the periods of time that surface sites were affected by the lake-breeze circulations on July 15 and August 9, 2015.

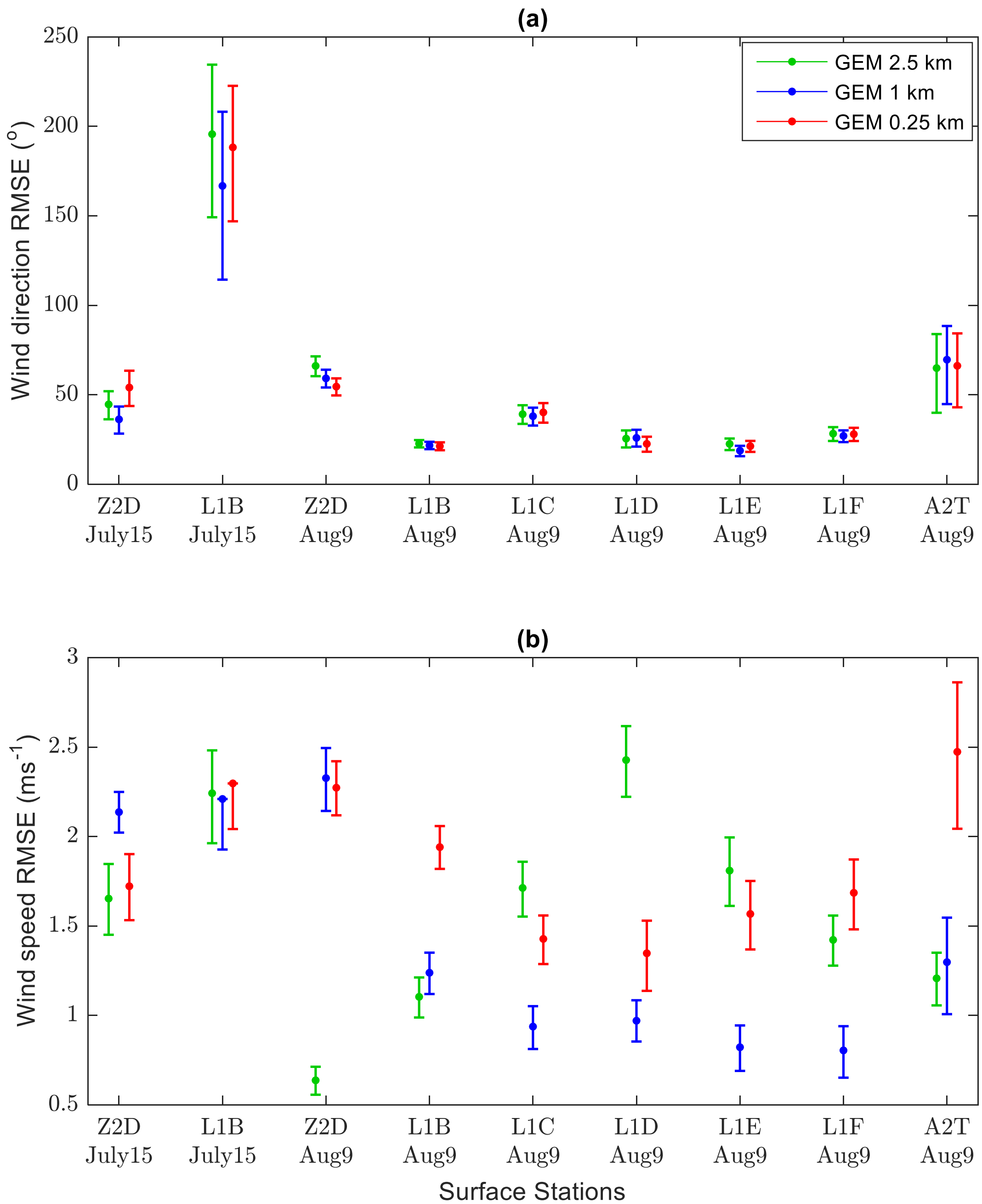

Fig. 20. The same as Fig. 19, except for (a) horizontal wind direction (°) and (b) horizontal wind speed (ms^{-1}).